NUMERICAL MODELLING OF AN OFFSHORE PIPELINE LAID FROM A BARGE

by

M.F. SNYMAN

B.ING (Siviel) (RAU)

A thesis submitted in partial fulfilment of the requirements for the degree of Master of Science in Engineering.

Department of Civil Engineering.

University of Cape Town.

September 1988

to my parents

ACKNOWLEDGEMENTS

I would like to express my gratitude to the following:

Dr. Colin Mercer for his guidance and constructive criticism during my study.

Dr. Howard Pearce who introduced me to the problem.

The SANCOR National Program of the Foundation for Research and Development for financial support.

Jack Vos and Helena du Toit who kept the MicroVAX going.

Antoinette for her love, patience and support.

Finally, my family, and especially my parents, for their continuous support and interest in my studies.

ABSTRACT

This thesis addresses some of the issues involved in using numerical methods to simulate the laying of an offshore pipeline, the objective being to contribute to the expertise of the South African offshore technology. Of particular interest is the prediction of the stresses in the pipe during such an event.

The thesis concentrates on the use and suitability of the finite element method to simulate the important aspects of the pipelaying problem. ABAQUS, a nonlinear general purpose finite element code, was chosen as numerical tool, and nonlinear effects such as geometry and drag, as well as contact and lift-off at the boundaries, are included in the models.

The analysis is performed in two parts: in the static analysis the displaced equilibrium position of the pipeline under self weight, buoyancy and barge tension is sought, whilst the response due to wave action and barge motion is of interest in the dynamic analysis.

Numerical experiments show the suitability of ABAQUS to model the behaviour of slender structures under both static loads and dynamic excitations.

Contents

List of Figures

List of Tables

NOMENCLATURE

Convention used

Uppercase boldface characters represent matrixes (eg. $\mathbf{M}$)

Lowercase boldface characters represent vectors (eg. $\mathbf{v}$)

Upper and lowercase italic characters represent scalars (eg. C and c)

Uppercase symbols

A	Constant
$\mathbf{C}$	Structural damping matrix
C_a	Pressure gradient coefficient
C_d	Drag coefficient
C_i	Inertia coefficient
C_m	Added mass coefficient
D	Pipe Diamter
F_f	Total fluid force on a slender member
F_d	Drag force
F_i	Inertia force
$\mathbf{K}$	Structural stiffness matrix
$\mathbf{K}^e$	Element stiffness matrix
$\mathbf{K}^{f_x}$	Foundation stiffness matrix in horizontal direction
$\mathbf{M}$	Structural mass matrix

Lowercase symbols

a	Acceleration of a fluid
$\mathbf{a}$	Acceleration vector of a fluid
c_d	Drag coefficient
c_m	Added mass coefficient
c_i	Inertia coefficient
$\mathbf{f}$	External load vector
$\mathbf{f}_s$	Static load vector
$\mathbf{f}_f$	Fluid load vector

$k_{11}^{f_x}$	Foundation stiffness term in horizontal direction
t	Time
v	Velocity of a fluid
$\mathbf{v}$	Velocity vector of a fluid
x	Displacement of a structural member
$\mathbf{x}$	Displacement vector
$\dot{x}$	Velocity of a structural member
$\dot{\mathbf{x}}$	Velocity vector of a structural member
$\ddot{x}$	Acceleration of a structural member
$\ddot{\mathbf{x}}$	Acceleration vector of a structural member

Special Characters

ρ	Fluid density
σ_v	Standard deviation of velocity
ω	Natural fraquency
ϕ	Phase angle of a wave

1 INTRODUCTION

Submarine pipelines are needed to transport oil or gas from a rig to either land or tankers. These pipelines must be laid on the seabed at extreme depths and are often exposed to severe environmental conditions. High stresses, and ultimately failure, may occur and since enormous costs are involved, an analytical or numerical analysis is essential in order to understand the complex behaviour.

The mechanics of the pipelaying problem are characterised by nonlinearities arising from large displacements, contact between the pipe and barge support, contact between the pipe and seabed, and the nonlinear drag force. An additional complication is the unknown suspended length of the pipe at the beginning of the analysis. Since closed form solutions are only possible for relatively simple cases, a numerical analysis must be performed. Of particular interest is the finite element method, which provides the most developed and general numerical tool available to the analyst.

The underlying objective of the study is to contribute to the expertise in South African offshore technology. In this thesis the emphasis is placed on increasing the understanding of both the mechanics and computational aspects concerned. This is achieved by firstly ascertaining the mechanics of the physical problem, and the analytical and numerical solution techniques used in other studies, and secondly, to obtain experience with some aspects of the pipelaying problem using a particular numerical solution technique.

The literature study summarises the relevant technology, mechanical aspects and numerical solutions available for the problem. Numerical problems inherent to the problem, and experienced by other researchers, are identified. It was concluded that the finite element method is the most advantageous solution method.

A general purpose nonlinear finite element code was then used to ascertain to what degree the results obtained from a such a code agree with reported results, identify problem areas, seek solutions to them and report on the suitability of general purpose codes, such as ABAQUS, to model the important aspects of the pipelaying problem. The basic philosophy was to keep the models as simple as possible, but of sufficient complexity to adequately simulate the physical problem.

Chapter 2 reviews the literature, whilst Chapter 3 discusses the capabilities

and limitations of the nonlinear finite element code ABAQUS (Version 4.6), used in this study.

A large number of numerical experiments were performed in order to develop a suitable finite element model that includes all the components that characterise the pipelaying problem. Some of these models and the results obtained are presented in Chapter 4

Guidelines for the structural analyst, which will be of assistance in providing reliable results relatively quickly, are given in Chapter 5. These principles were also applied to an example of a gas-pipeline to be laid in South African waters. A description of the model used, and some of the results obtained are given in Appendix A.

1.1 PIPELAYING TECHNOLOGY

Before proceeding with a discussion and a review of the modelling techniques for offshore pipelines found in literature, a brief discussion of the technology involved is necessary.

The submarine pipe consists of a steel lining covered with a concrete coating. The coating serves as protection, and provides weight needed for stability against currents on the seabed.

A variety of methods exist for installing an offshore pipeline. These methods include the laybarge methods, reel barge methods and various tow and pull methods.

The conventional laybarge method (Fig. 1.1) is the most common method of installation. In this method, short sections of pipe are welded together on a barge to form a continuous pipe. The barge is usually kept in position with a system of anchors. By changing the anchors' position, the barge moves forward and the pipe is lowered onto the seabed in a long, gentle S-curve. To prevent the pipe from buckling, an axial force is applied to it by tensioning devices on the barge.

A flexible tail-like ramp, called the *stinger*, is attached to the barge to partially support the suspended length of the pipeline. The articulated stinger is perhaps the most effective and widely used. It consists of elements hinged together with frictionless rollers, positioned in a V-shape along the stinger, to support the pipeline. Each element has its own buoyancy pontoon which can

be controlled from the barge. The stinger configuration can then be varied by changing the buoyancy of individual elements.

Pipe stresses for a specific case are kept within prescribed limits by choosing a suitable barge tension and stinger configuration. These stresses can also be reduced by changing the submerged weight. This can be accomplished by using temporary buoys at intervals along the pipe length.

In addition to the conventional method, the pipe can be laid onto the seabed by means of the J-laybarge method (Fig. 1.2). This technique involves running the pipeline through the centre of the vessel on a vertical or inclined derrick. The idea with the J-laybarge method is to avoid using a stinger, which is a weak structural component. The disadvantage of the derrick is its orientation. The inclination causes difficulties in handling the pipe which results in slower laying than the conventional laybarge method.

The reel barge method of laying a pipeline uses a continuous length of pipe coiled onto a reel. The pipe is assembled onshore and transported to the site where it is unwound into the required position. Its application is limited to short, small diameter pipes laid in relatively shallow water depths.

Various tow and pull methods exist: in the bottom-pull method the pipe is constructed onshore and then pulled along the seabed to its final position by means of a tow vessel. Alternatively, the pipe can be towed between two barges to the site. In this method, the pipeline is suspended, and does not have to move over a rocky ocean bottom.

Weather plays an important role in pipelaying. Pipelaying becomes difficult and stresses may increase to unacceptable levels in stormy weather. It then becomes necessary to stop the laying operations and lower the pipe onto the seabed. The process of lowering the pipe onto the seabed and winching it up to the barge again, is called the *abandonment* and *recovery* process.

In order to lay pipelines effectively and economically, it is important to be able to model the abovementioned construction methods numerically. In this study we will devote our attention to pipelines laid with the conventional laybarge method. The J-laybarge method, the reel method and the tow and pull methods are only used in exceptional cases and will not be considered. In addition we are only interested in the global response of the pipeline due to environmental loads. Localised effects such as buckling of the pipeline or ovalisation of the cross-section are outside the scope of this study.

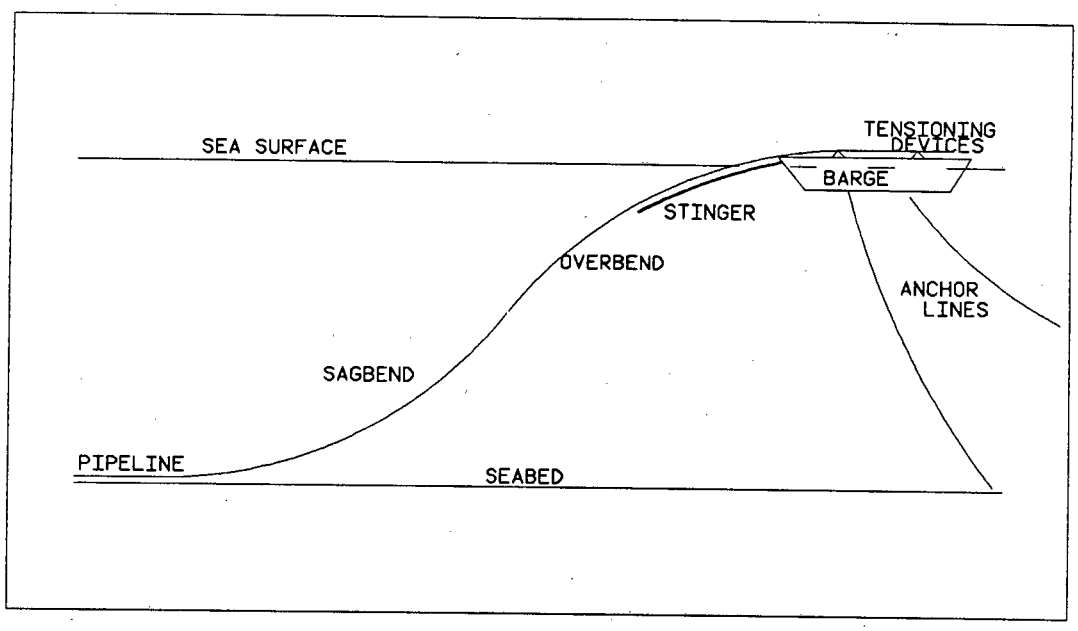

Figure 1.1: Conventional Laybarge Method

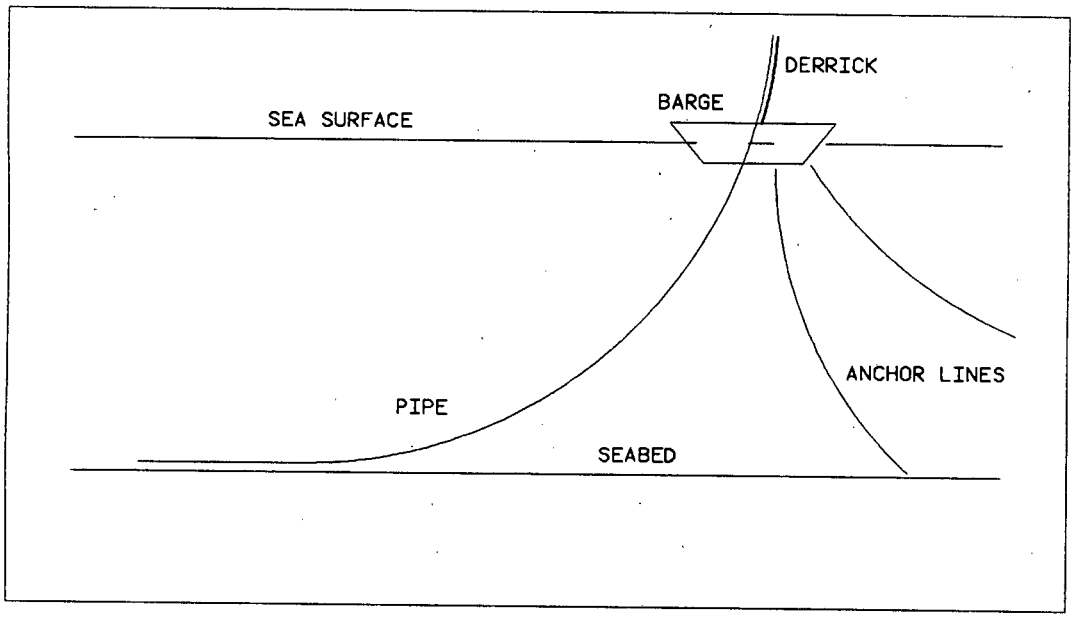

Figure 1.2: J-Laybarge Method of Laying

2 ANALYSING THE SYSTEM (A REVIEW)

Analysis of a structural engineering system requires the following basic steps [2] [22]: the first step is to identify all the loads that act on the system and to determine the type of analysis required (eg. static or dynamic). The next step is to idealize the system in a form that can be analysed. This is followed by the formulation of the system governing equations and solution of the differential equations subjected to the appropriate boundary conditions. Where discreet methods are used, solution of the resulting algebraic equations and interpretation of the results completes the analysis.

This chapter reviews the literature of the analysis of pipelines laid from a barge. The chapter is divided into the various steps described above as follows: Section 2.1 discusses the different loading effects, Section 2.2 the methods available for analysis, Section 2.3 the assumptions, Section 2.4 and 2.5 the governing equations and their solutions and Section 2.6 the solution of the algebraic equations.

2.1 LOADING EFFECTS

The static loads (Fig. 2.1) consist of the self weight, buoyancy, barge tension and forces resulting from currents, whilst the dynamic loads (Fig. 2.2) consist of wave forces on the pipeline and forces resulting from barge motions. The combined effects of buoyancy and self weight are usually replaced by the submerged weight.

The reaction forces are the seabed and stinger reactions. The seabed reaction can be seen as a continuous flexible support or elastic foundation and the stinger support as concentrated loads exerted (perpendicular to the pipe curve) at discrete points along the stinger length.

Waves, currents and barge motions account for most of the loading on the pipeline and hence are of fundamental importance to the response of the pipeline. The fluid-structure interaction due to these effects introduce two forces, the drag and inertia forces, on the structure. The inertia is understood to be that part of water oscillating together with the structure and the effect is that of adding additional mass to the structure. The drag force is due to the viscous effect of the fluid, and is often referred to as hydrodynamic damping since the effect of the force is to damp out structural motion.

The following sections discuss some of these loads in more detail.

2.1.1 Wave theories

The unpredictable and irregular pattern of wave crests and troughs on the sea surface requires a complex mathematical description, best described by a random or statistical function. Various linear and higher order wave theories exist, describing the propagation of a simple design wave in a deterministic way. These theories are derived by solving the Navier-Stokes equation, which is a partial differential equation that describes the motion of a fluid particle. The differences between them depend on the type of approach followed to approximate the unknown free surface position or boundary condition.

Stokes and Airy wave theories are commonly used in offshore analysis. The equations for these theories are solved by expressing the surface boundary with analytical perturbation methods. In the case of the Airy theory only the first term of a Taylor series expansion is used to approximate the surface.

The linear Airy wave theory is only valid in deep water. It describes an oscillatory wave where the wave amplitude is small compared to the wave length. The higher order Stokes theory can be used to predict characteristics of large amplitude waves more accurately.

Other wave theories, such as the Cnoidal wave theory, can be used to describe long, small-amplitude waves propagating in shallow water.

A stochastic model that describes random wave actions can be developed by superposition of a large number of simple waves, each having a different and random phase, amplitude, velocity and direction. From this, certain statistics of the sea surface and a spectral representation of the sea state can be obtained. The Pierson-Moskowitz and JONSWAP are two of the commonly used wave spectra. This probabilistic approach allows results for maximum stresses and displacements of the structure to be obtained within a certain confidence range, and is accepted as a more realistic wave model [8].

2.1.2 Laybarge Movements

In addition to the direct action of waves on the structure, waves also give rise to barge motions. Since the sea surface consists of irregular waves, the imposed barge motions are also random. The six independent barge motions

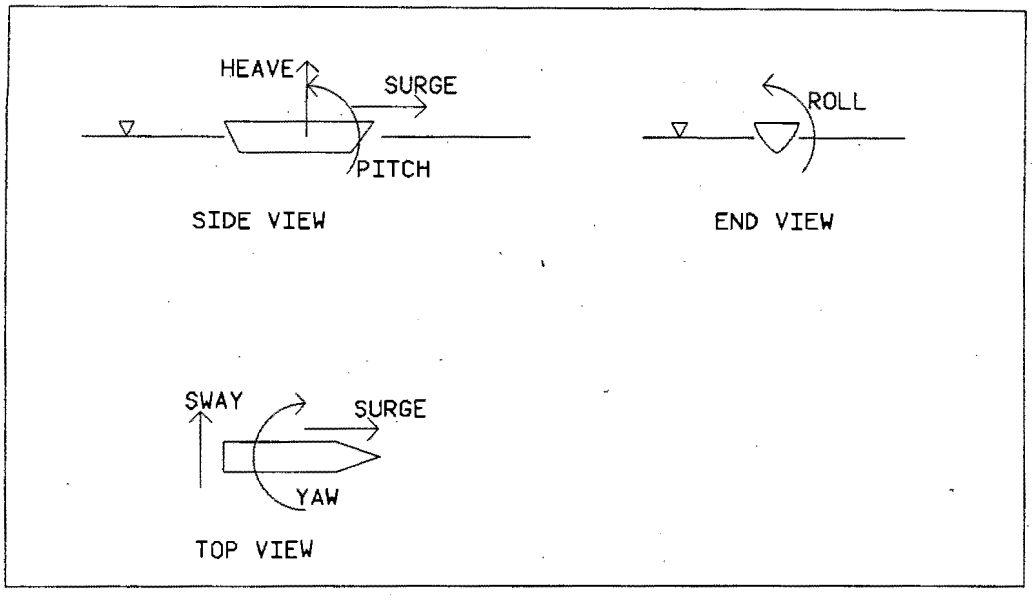

Figure 2.3: Barge Motions

(roll, pitch, heave, sway, yaw and surge), shown in Figure 2.3, can also be represented in either a deterministic or probabilistic way as described in the previous section.

Brewer and Dixon [9] have investigated the sensitivity of a tensioned pipeline laid by the J-laybarge method, to the two dimensional laybarge motions, namely surge, heave and pitch. The remaining three motions have relatively little influence and are usually neglected. They used a quasi-static analysis, neglecting the fluid-structure interaction, and concluded that the stresses near the seabed part of the pipe are mainly influenced by surge and to a lesser degree by heave. These effects are especially dominant in shallower and intermediate water depths and the effect diminishes with increasing depth. The stress near the top end of the pipe is mostly influenced by pitch. This effect becomes more dominant in deeper waters and when the tension is large.

Hall [25] investigated the response of the pipeline due to a sudden heave motion in a deterministic way. The results show how the drag force damps out structural motion.

The mode corresponding to the lowest natural frequency of the pipe, is a sway mode. The frequency of this mode is determined by the pipe span

geometry and barge tension. Flexural and torsional rigidity have relatively little influence.

2.1.3 Morison's equation

Forces resulting from waves, currents and barge motions can be divided into forces exerted on large bodies where diffraction must be taken into account, and forces exerted on slender members. The pipeline is a very slender member and diffraction does not have any effect on forces.

The two main identifiable forces on a slender member are the drag and inertia forces. Drag is due to the effects of viscosity of the fluid, and is assumed to be proportional to the square of the relative fluid-structure velocity. The inertia force, which is independent of viscosity, can be thought of as being composed of two parts: firstly a hydrodynamic or added mass of the member, representing a weighted average of the mass of the water that is excited in phase with the acceleration of the moving member , and secondly, an inertia force due to variation of pressure gradient within the accelerating fluid.

The force per unit length at depth z and time t, on a slender member, may therefore be written as follows:

$$F_f(z,t) = F_i + F_d \tag{2.1}$$

with the drag force given as:

$$\begin{aligned} F_d &= C_d(v-\dot{x})\,|(v-\dot{x})| \\ &= \frac{1}{2}\rho c_d D(v-\dot{x})\,|(v-\dot{x})| \end{aligned} \tag{2.2}$$

and the inertia force as:

$$\begin{aligned} F_i &= C_i\,(a-\ddot{x}) \\ &= (\frac{1}{4}c_m\rho\pi D^2 + \frac{1}{4}\rho\pi D^2)\,(a-\ddot{x}) \\ &= \frac{1}{4}\rho\pi D^2 c_i\,(a-\ddot{x}) \end{aligned} \tag{2.3}$$

where:

F_f = Force due to fluid interaction
F_d = Drag force
F_i = Inertia force

C_i = Inertia coefficient
C_d = Drag coefficient
v = Velocity of fluid
a = Acceleration of fluid
$\dot{x}$ = Velocity of member
$\ddot{x}$ = Acceleration of member
c_d = Drag coefficient
c_i = Inertia coefficient
c_m = Added mass coefficient
D = Pipe diameter
ρ = Fluid density

Some uncertainty is involved in selecting the drag coefficient c_d and the added mass coefficient c_i. They are functions of the Reynolds number, Keulegan-Carpenter number and the roughness of the pipe. It has been shown that especially the drag force varies considerably with different values of Reynolds and Keulegan-Carpenter numbers [8] [12]. Since it is difficult to determine these values in practice, it is also difficult to select proper drag and inertia coefficients.

Another uncertainty is the selection of a wave theory. Hogben and Standing [8] compared forces, using waves with the same height and period, obtained from Airy and Stokes theories. They have shown that inertia forces calculated from the two theories differs by 7 % whereas the drag contribution differs by 13 %. They conclude that the linear theory is adequate for very slender, drag dominated members near the surface of the water.

2.1.4 Stinger and Seabed Support Conditions

The seabed provides a flexible support, and the stinger discrete supports at the roller positions. Contact and lift-off occur during dynamic excitation, and the reaction forces at the boundaries change continuously with time.

The seabed has been modelled as a horizontal, rigid boundary by most researchers. This means that the bending moment in the pipe is zero at the seabed and a pinned condition can be assumed.

Brewer et al. [9] investigated a negative and positive sloping seabed. They concluded that if the slope is negative (lying from deep to shallow water), the maximum static bending stress will be less than for a horizontal slope at

the same depth.

Hall et al. [25] used a visco-elastic bilinear support to model the seabed. A reaction force was assumed to be applied normal to the bottom surface and proportional to the depth of penetration for parts of the pipeline in contact with the bottom. These forces were nonexistent for a lift off situation. They showed that pipe stresses increase with rigidity of the seabed.

Larsen [35] included strain energy in his model due to a continuous linear elastic seabed.

Few researchers have included the stinger. They have ignored the stinger by assuming that the pipe stays in contact over the full stinger length. This imposes a known curvature and therefore a known bending moment in the pipeline along the stinger length. The stinger can then be replaced by applying this bending moment as a boundary condition at the stinger tip. Only the sagbend curve is then modelled. This method simplifies to a model which is equivalent to the J-laybarge method.

More accurate stinger models are given in Larsen [35], Cowan et al. [14] and Palmer et al. [41]

2.2 METHOD OF ANALYSIS

Two classes of methods are available for analysing system response [8]. If inertia forces are unimportant, a static analysis is sufficient. When inertia effects are significant, dynamic analysis is necessary. A dynamic analysis can be performed in either the frequency domain or time domain. Frequency domain analysis concentrates on steady-state solutions and transient effects are neglected. A disadvantage is that only linear behaviour can be considered. The time domain uses some time step integration technique, in which case transient effects as well as nonlinearities can be considered.

Owing to computer time savings, the frequency domain analysis is usually preferred; but time domain analysis is needed when nonlinear effects such as drag have to be considered and nonlinear wave theories have to be used.

Frequency domain methods can be divided into deterministic and probabilistic methods. In the deterministic method the sea state is assumed to consist of a simple design wave of given amplitude and period. This wave is usually taken as the maximum wave corresponding to a storm with a hundred

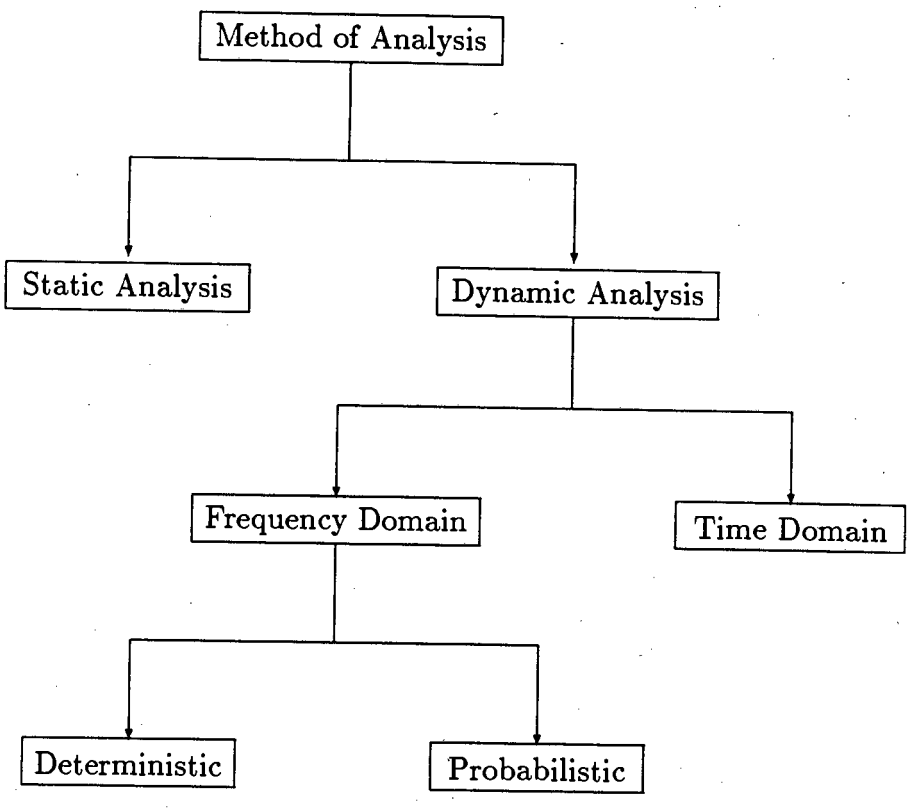

Figure 2.4: Method of Analysis

year return period, which may act on the structure during its life time. The second approach is to express all the sea states that will occur during the life of the structure by means of spectral methods using probabilistic theory. In this case the response of the structure is also expressed statistically, and results can be obtained within a certain level of confidence.

Figure 2.4 demonstrates the methods diagrammatically.

2.3 SYSTEM IDEALIZATION

Normally in structural analysis, we assume that both the displacements and strains developed in the structure are small. This means that the geometry of the structure essentially remains unchanged during the loading process and that first order, linear strain, approximations can be used. In addition we assume that the boundary conditions remain unchanged during application

of the loads. These assumptions lead to linear differential equations.

However, in some problems (eg. the pipelaying problem) these assumptions do not hold, and higher order approximations which lead to nonlinear differential equations [18] [3] must be introduced. Three types of structural nonlinearity exist. Firstly, material nonlinearity, where the constitutive relations are nonlinear. Secondly, geometric nonlinearity, which means that the structure has undergone deflections large enough to cause significant changes in geometry, and that the equations of equilibrium must be formulated for the deformed configuration. Finally, boundary nonlinearity, where the boundary conditions change during application of the load.

In offshore analysis, pipelines and risers normally undergo large displacements, and geometric nonlinearity must be used. It is usually assumed that the stresses and strains remain within the elastic limits and linear constitutive relations are therefore sufficient. An exception to this is the model of Bergan and Mollestad [5]. They used an elasto-plastic material model which included kinematic and isotropic hardening.

Dynamic response of the system also involves nonlinearities from hydrodynamic damping, the pipe-stinger interaction and pipe-seabed interaction. Hydrodynamic damping can be seen as a force nonlinearity whilst the contact between pipe-seabed, and pipe-stinger are boundary nonlinearities. These nonlinearities, especially contact and lift off, cause difficulties in determining a solution for the governing equations, and to simplify the boundary conditions, most researchers have used pinned or fixed support conditions.

Another feature of the problem is that the length of the suspended pipeline is unknown at the beginning of the analysis. This means that the point where the boundary conditions act upon is unknown. In this sense the problem is a free boundary problem, in many ways analogous to free surface problems in fluid mechanics.

The flexibility of the pipeline and weak coupling between the boundary conditions at the two ends influences the convergence of most numerical methods and a solution is often difficult to obtain [44] [35].

2.4 STATIC GOVERNING EQUATIONS

The governing equations of a system can be derived by using either the direct method or variational principles [2]. The direct method accomplishes

the formulation of element relationship by direct combination of the equations of equilibrium, the strain-displacement equations and the constitutive equations. Variational principles are based on finding the extreme value of an energy function of the system. The advantage of the variational method above the direct method lies in the way in which some of the boundary conditions are generated. Both methods, however, lead to the same governing equations. Direct methods have been used by most authors. Exceptions are the models of Larsen [35] and Kirk [32].

The first attempt to solve the two-dimensional static configuration of the pipe under self weight, buoyancy and tension was achieved by Dixon and Ruthledge [9]. They derived a second-order differential equation in polar coordinates (which they expressed in non-dimensional form) by considering a small beam element subjected to self weight and buoyancy forces only.

Mathematically the pipeline can be best described as a thin rod with large nonlinear deformations. Using classical rod theory, Konuk [33] [34] and Brown [10] have derived general three dimensional, large angle models which include twist.

Solution of the governing equations subjected to the boundary conditions follows. The nature of the governing equations and boundary conditions (their nonlinearity) makes analytical solutions impossible and numerical methods must be employed. An exception is the early catenary solution which is mathematically expressible in closed form. This method is still being used to obtain preliminary design results and as a trial solution in numerical methods.

Some of the more recent numerical solutions include forward integration, successive integration, finite differences and finite elements. A common problem with these methods is to obtain a convergent solution in extreme cases. This problem can be overcome if a good trial solution, such as the catenary solution, is known.

The following sections discuss these solutions in more detail.

2.4.1 Catenary Solution

The simplest problem to be solved is that of determining the static configuration of the two dimensional pipeline, in which the suspended pipe, the barge and the line of the pipe, all lie in the same vertical plane. Both ends are

considered pinned and the problem can be regarded as a two-point boundary value problem [49].

In the first attempt to solve the governing equation, the bending stiffness term was neglected. This is analogous to the governing equation of a cable loaded by its own weight. The solution to this problem is the classic nonlinear catenary.

The pipeline approximates this shape over most of its length and only deviates from it near the ends. This is due to the bending stiffness being neglected, and the boundary conditions which are not compatible with those of a natural catenary. However, it is a good approximation, particularly if the tension is large, the water deep and the pipe small and heavy.

2.4.2 Stiffened Catenary Solution

Plunkett [45] made the first attempt to solve the governing equation including the bending stiffness term. He recognised it as a singular perturbation problem and derived asymptotic expansions to describe the shape taken up by a stiffened catenary. He applied the method to drill strings and stiffened cables as examples.

The method is only valid if the tension has more influence on deflection than the bending stiffness over most of the length. The solution consists of two parts:

1. a base solution which is valid over most of its length but not satisfying the boundary conditions,
2. a boundary region at each end which gives the transition from the main modified catenary, to the imposed boundary conditions of slope or moment.

Dixon and Ruthledge [19] applied Plunkett's [45] expansions to the analysis of a pipe being laid by the J-method. This method has also been used by Larsen [35] and Brewer et al. [9].

Unfortunately, these solutions are difficult to apply, since a group of implicit equations relate the quantities that are likely to be prescribed in a particular problem, to those that are likely to be wanted as results. The method is also difficult to apply when the pipe is laid by the conventional laybarge method

(Fig. 1.1), and when forces resulting from stingers, buoys and currents must be considered. In addition, the stiffened catenary solution is only valid for pipelines with small bending stiffnesses or pipelines laid in deep water.

2.4.3 Forward Integration

The two-point boundary value method can be transformed into an initial-value problem and solved by iteration. This can be accomplished by the forward integration method, which consists of constructing the pipeline curve, starting from the seabed and gradually increasing upwards by adding beam elements at the end of the previous one.

Brando and Sebastiani [7] and Rammant and Backx [46] used this method. They derived the governing equations for an element, loaded by buoyancy and an axial tensile force, and based their theory on small angle bending assumptions.

Both researchers assumed the pipe to be in continuous contact with a stinger with known radius of curvature, imposing known kinematic boundary conditions at the stinger end. They considered the other end supported on a horizontal non-compressible seabed. The reaction forces applied at the point of contact with the seabed consist therefore of a known axial force, zero bending moment (since curvature is zero for horizontal bottom) and an unknown shear force.

Their procedure is as follows: starting with the known reactions and assumed shear force at the bottom, the total large angle deflection curve can be obtained by adding small angle beam elements at the end of the previous one. Each time a beam element is added, the total static equilibrium shape of the curve is obtained iteratively. Different bottom shear forces must be used. The correct pipe curve is the curve that satisfies the compatibility requirements at the barge end.

The advantage of this method over the conventional finite differences or finite element method is that one does not have to assemble the beam stiffnesses in a global stiffness matrix, nor solve large systems of nonlinear equations. The disadvantages lie in the necessity of having to build many possible pipe curves to find the unique one, and that small changes in shear force often induce very large changes in displacement at the barge end. Another drawback of the method is that for long, flexible pipelines, convergence is very slow and even unattainable because of the weak coupling between the two ends.

2.4.4 Successive Integration

Pederson [44] solved the equations numerically by successive iterations. Mathematically, the method is based on a series of formal integrations. The procedure is as follows: an initial deflection curve is estimated, the loads on the pipe associated with this curve are determined, and based on these loads a new deflection curve is found. This shape is then used in the next iteration to calculate new loads. This procedure is repeated until convergence is obtained and the true length and shape of the pipeline is found.

The advantage of the method lies in the low computer time and the flexibility of the method. For instance, different types of stingers, the abandonment and recovery operations and the behaviour of cables have been modelled.

The disadvantage lies in the convergence problems encountered in extreme cases, such as pipelines in very deep water or with small bending stiffnesses.

2.4.5 Finite Difference Methods

In the finite difference technique, the pipe is divided into equal panel lengths. The governing equation for each panel is then represented in the form of a finite difference equation, and written for all the interior nodes. The boundary conditions are also presented in terms of finite difference equations, and are written for the end nodes.

Because the touchdown point of the pipe relative to the barge is unknown, trial and error must be used to satisfy the boundary conditions which are functions of this unknown length.

The convergence of this technique often depends on the initial trial displaced profile selected. Most authors have used the catenary solution as an initial estimate. This is a reasonable choice, not only because the pipe approximates this shape over most of its length, but also because the catenary is mathematically expressable in a closed form, thus eliminating large data structures to describe the initial curve.

Finite difference techniques have been used by Dareing and Neathery [15], Palmer et al. [41], Datta and Basu [16], Hall and Healy [24], Bryndum and Colquhoun [11] and Datta [17].

Dareing and Neathery [15] derived coupled nonlinear differential equations

which they solved by Newton's method. Their method involves linearizing the governing equations by truncating a Taylor series. The linearized equations are then expressed in terms of finite differences. They used the catenary solution as an initial trial solution.

Palmer et al. [41] expressed the nonlinear equations in terms of a five point finite differences scheme with all the nonlinear terms on the right hand side and the linear terms on the left hand side of the equation. The first approximate solution is then obtained by setting the right hand side to -1. This solution is then used to construct a first approximation of the right hand side, and the procedure is then repeated to find a successive approximation.

Datta and Basu [16] investigated two starting curves for different boundary conditions of the suspended pipeline. In the first case they used a third degree polynomial with zero slope and zero moment at the seabed end, and zero deflection and specified moment at the laybarge end. In the second case a second degree parabola is assumed with zero slope and specified moment at the seabed end and zero deflection at the stinger end. They solved the simultaneous equation using the Newton-Raphson method and concluded that a relatively coarse mesh gives sufficiently accurate results and that the iteration method has rapid convergence.

Hall and Heally [25] investigated pipes laid with temporary buoys to reduce the self weight and hence the pipe tension and barge thrust needed. This is analogous to a long continuous beam having a variable weight and tension. They used an initial trial catenary solution and solved their simultaneous equations by successive over relaxation.

Datta [17] used a finite difference technique to model abandonment and recovery. He included drag forces due to currents in his model and solved the resulting simultaneous equations using a modified Newton's method.

Finite difference methods are not very convenient since general algorithms cannot be written and must therefore be modified for different cases. This is a problem, especially in a design context, where time is a critical factor.

2.4.6 Finite Element Methods

The finite element method offers the most versatile way of analysing a structural system. The problem is to find the unknown displacements by an

iterative solution of the equilibrium equitions given by:

$$\mathbf{K}(\mathbf{x})\mathbf{x} = \mathbf{f}(\mathbf{x}) \tag{2.4}$$

Details of the method can be found in most finite element text books [2] [3] [22] [50] and are not discussed here.

One of the method's most advantageous features is its generality. Modern day finite element codes offer the user a large number of analysis procedures, element types and other special features, allowing analysis of a variety of problems. Another advantage is that the dynamic analysis is just an extension of the static analysis, and the same discretization and element formulation can be used.

Other advantages include the capability to model the boundaries in more detail than is allowed by other methods, and the capability to increase the accuracy in certain areas of interest by varying the element length [14].

Numerical difficulties, however, often occur, and are due to the strong nonlinearities introduced by the boundary conditions and the properties of the beam elements chosen. The stiffness matrix for the beam-column element [35] is obtained by summation of the ordinary beam element and a geometric stiffness matrix proportional to the axial force in the element, formally expressed by:

$$\mathbf{K} = \mathbf{K}_b + \mathbf{p}\mathbf{K}_g \tag{2.5}$$

The axial force $\mathbf{p}$ is unknown and is found from the relative axial displacements of the nodes. In the pipe laying problem the axial stiffness is large compared to the bending stiffness and consequently, the stiffness matrix becomes strongly dependent on the unknown axial deformations. This is an unfavourable situation and causes numerical difficulties.

The bottom and stinger interaction with the pipeline introduce another strong nonlinearity. Contact of the pipeline with the seabed and stinger causes an instantaneous change in the stiffness matrix, which can cause numerical difficulties. A way to overcome this problem is to represent the seabed and stinger with relatively soft springs [35].

2.5 DYNAMIC GOVERNING EQUATIONS

The equations of motion for a structure are given as follows:

$$\mathbf{M}\ddot{\mathbf{x}} + \mathbf{C}\dot{\mathbf{x}} + \mathbf{K}\mathbf{x} = \mathbf{f}(t) \tag{2.6}$$

where:

$\mathbf{M}$ = Structural mass matrix
$\mathbf{C}$ = Structural damping matrix
$\mathbf{K}$ = Structural stiffness matrix
$\mathbf{f}(t)$ = External load vector at time t
$\mathbf{x}$ = Displacement vector
$\dot{\mathbf{x}}$ = Velocity vector
$\ddot{\mathbf{x}}$ = Acceleration vector

An important characteristic of the pipeline problem is the fluid-structure interaction. This means that the external load vector $\mathbf{f}(t)$ will have contributions due to barge movements and wave motions in addition to the static forces (buoyancy and tension), hence:

$$\mathbf{M}\ddot{\mathbf{x}} + \mathbf{C}\dot{\mathbf{x}} + \mathbf{K}\mathbf{x} = \mathbf{f}_s + \mathbf{f}_f \tag{2.7}$$

where $\mathbf{f}_s$ represents static forces and $\mathbf{f}_f$ the dynamic forces resulting from fluid-structure interaction (Section 2.1.3).

The inertia force, which is a function of acceleration, is usually added to the structural mass matrix on the left hand side of Equation 2.7. This can be visualized as a weighted average of the mass of water oscillating together with the structure. Equation 2.7 can then be rewritten as:

$$(\mathbf{M} + \mathbf{C}_i)\ddot{\mathbf{x}} + \mathbf{C}\dot{\mathbf{x}} + \mathbf{K}\mathbf{x} = \mathbf{f}_s + \mathbf{f}_d + \mathbf{C}_i\mathbf{a} \tag{2.8}$$

Damping of pipeline oscillation is mainly caused by the relative motion between pipe and fluid and is called hydrodynamic damping or drag. This force is proportional to the square of velocity (Eq. 2.2). Since frequency domain solutions assume linear response, the drag force must be linearized. The non-linear drag term is usually replaced by a linear part and an error function. The error function can then be minimised and ultimately neglected. This can be done by the least square method where the velocity is expressed by a Gaussian probability distribution with zero mean [8] [25]. The linearized drag force is then written as:

$$\begin{aligned} \mathbf{f}_d &= \sqrt{8/\pi}\,\sigma_v\,\mathbf{C}_d\,(\mathbf{v} - \dot{\mathbf{x}}) \\ &= \bar{\mathbf{C}}_d\,(\mathbf{v} - \dot{\mathbf{x}}) \end{aligned} \tag{2.9}$$

where σ_v is the standard deviation of the velocity. This term can then be added to the damping matrix to obtain the following equation:

$$(\mathbf{M} + \mathbf{C}_i)\ddot{\mathbf{x}} + (\mathbf{C} + \bar{\mathbf{C}}_d)\dot{\mathbf{x}} + \mathbf{K}\mathbf{x} = \mathbf{f}_s + \mathbf{C}_i\mathbf{a} + \bar{\mathbf{C}}_d\mathbf{v} \tag{2.10}$$

In the case where a nonlinear drag force is required, it must be introduced on the right hand side of Equation 2.8 as part of the forcing function, hence:

$$(\mathbf{M} + \mathbf{C}_i)\ddot{\mathbf{x}} + \mathbf{C}\dot{\mathbf{x}} + \mathbf{K}\mathbf{x} = \mathbf{f}_s + \mathbf{C}_i\mathbf{a} + \mathbf{C}_d\,(\mathbf{v} - \dot{\mathbf{x}})\,|\mathbf{v} - \dot{\mathbf{x}}| \quad (2.11)$$

Two methods exist for solving Equations 2.10 and 2.11. They are the linear frequency domain and nonlinear time domain methods.

2.5.1 Frequency domain

Analysis in the frequency domain assumes harmonic response due to force excitation. The solution to Equation 2.10 is obtained by assuming a response of the form:

$$x = Ae^{i(\omega t + \phi)} \quad (2.12)$$

where:

x = Displacement
A = Constant
i = Complex number ($i^2 = -1$)
ω = Natural frequency
ϕ = Phase angle

With this assumption the problem reduces to an eigenvalue problem where the eigenvalues are frequencies and the eigenvectors the corresponding mode shapes.

Frequency domain analysis can be performed in either a deterministic or probabilistic way (section 2.2). Details of these methods can be found in most structural dynamic texbooks [4] [13] [21] [43].

In the derivation of this method, the principle of mode superposition is employed, and it is therefore valid for linear behaviour only. The geometric nonlinearity is usually neglected by assuming small displacements of dynamic response relative to the static configuration. Stinger and seabed contact are neglected by assuming the ends fixed or pinned. In addition, the wave characteristics must be obtained from a linear theory such as the Airy wave theory, and the drag force must be linearized in the form described in the previous section.

This method has been used by most authors due to the simplicity, and the much cheaper run time in comparison with the time-domain solution.

One of the first attempts to analyse dynamic response was performed by Brewer and Dixon [9]. Only vessel motions were considered . Their analysis was based upon the stiffened catenary method.

Ovunc and Mallareddy [40] used a modified dynamic analysis where terms due to rotations are eliminated since inertial moments are neglected. They considered laybarge motions as the only dynamic loading.

Spectral analysis has been used by Kirk et al. [32], Cowan [14] and Rammant [46].

A serious drawback of the frequency domain method are the assumptions used to linearize the system. This can affect the accuracy dramatically and the method must be employed with care.

2.5.2 Time Domain

The nonlinear equation of motion, Equation 2.11, can be integrated numerically to obtain the solution. The most general method is the step-by-step integration procedure. In this approach, the response history is evaluated at successive short time intervals. The condition of dynamic equilibrium is established at the beginning of each interval and the response during a time interval is then evaluated by assuming a linear system having the properties determined at the beginning of the interval.

The step-by-step methods can be classified into two groups: the explicit and implicit methods. An explicit integration scheme solves the equilibrium condition at time t while the implicit solution is based on a solution time $t + \Delta t$. The explicit solutions have the disadvantage that they are unstable if the step length Δt is not selected sufficiently small, and the scheme is said to be conditionally stable. In unconditionally stable methods, such as most of the implicit methods, there is no restriction on the time step Δt, which is a time saving in comparison with the conditional stable method.

Examples of explicit methods are Euler time integration and central differences, whilst the Newmark-β method is an implicit method [4].

Hall and Healley [25] used an implicit Crank-Nicolson time average scheme where the equation of motion is expressed in the form of central differences.

They used a model which is able to simulate contact and lift off at the seabed. They concluded that harder soil conditions increase bending stress amplitudes, and that the sagbend region is the most critical zone. In addition, they compared the nonlinear solution with the linearized frequency solution. They concluded that the linearized solution yields conservative estimates of stress near the bottom, probably because the nodes are fixed, whereas the nonlinear simulation allows the nodes to lift off the seabed.

2.6 ALGEBRAIC EQUATIONS

In the stiffened catenary, forward integration and succesive integration methods, the solution of the governing equation subjected to boundary conditions reduces to a single algebraic equation which describes the total system.

In the finite difference and finite element methods the system is discretized and solution of the governing equation leads to a set of independent algebraic equations. In the linear case the equations have the form $\mathbf{Kx} = \mathbf{f}$, where $\mathbf{K}$ is the stiffness matrix, $\mathbf{x}$ the unknown displacement vector and $\mathbf{f}$ the external load vector. The unknown displacements can be solved by Gauss-elimination or an equivalent method.

In the nonlinear case the equations are of the form $\mathbf{K}(\mathbf{x})\mathbf{x} = \mathbf{f}(\mathbf{x})$ where both the stiffness and external loads are dependent on the unknown displacements x. Nonlinear algebraic equations are usually solved by dividing the nonlinear function into linear increments. Each linear increment is then solved in the usual way by using the properties determined at the end of the previous increment. Techniques include the incremental (Runge-Kutta), iterative (Newton-Raphson) and mixed methods.

2.7 CONCLUSION

This chapter reviewed the literature of analysis methods of pipelines laid from a barge. The various issues were placed in context by discussing them in the sequence that is normally taken in the analysis of any structural system. The advantages and disadvantages of the different analysis methods were discussed, and some of the numerical problems were identified.

The finite element method, which allows the user a large number of analysis procedures, element types and special features, appears to be the most ad-

vantageous solution method. ABAQUS is used to model the problem in this study. This code was chosen because it provides features such as a geometric analysis, elements to model contact of the pipe at the stinger and seabed, as well as different fluid forces that characterise the mechanics of the pipelaying problem.

It is apparent that few researchers have done a full nonlinear dynamic analysis, and that most of the nonlinearities have been linearized. Convergence problems, especially in extreme cases, were reported with most methods.

3 ABAQUS, A NONLINEAR FINITE ELEMENT CODE

ABAQUS is a general purpose nonlinear finite element code written by Hibbitt, Karlsson and Sorenson. In addition to stress analysis procedures, the code provides procedures such as heat transfer and eigenvalue buckling prediction.

A fundamental division of stress analysis problems is into static and dynamic response, the distinction being whether or not inertia effects are significant. ABAQUS provides algorithms to perform both static and dynamic analysis, and all three sources of structural nonlinearity (material, geometry and boundary) can be included.

This chapter reviews facilities (relevant to the pipeline problem) available in Version 4.6 of ABAQUS. The input required to define the model is discussed in Section 3.1, whilst the history input is discussed in Section 3.2. The discussion in this chapter is intended only as a summary of the capabilities and limitations of ABAQUS; the ABAQUS manuals [27] [28] [29] provide futher details.

3.1 MODEL SPECIFICATION

A finite element model consists of a geometric description, which is given by the elements, their nodes and a set of properties (such as material and cross sectional definitions) to describe the attribute of each element. Other parameters, describing interface elements, gap elements, springs, etc. may also be required. There may also be constraints that must be included in the model, boundary conditions that are to be imposed at the start of the analysis and environmental properties such as a fluid surrounding the model.

3.1.1 Elements

Beam elements are normally used to represent risers and pipelines in offshore analysis. All the beam elements in the ABAQUS library allow for both bending and stretching of the element, but no deformation (like ovalisation) of the cross-section.

Three interpolation schemes can be used: linear and quadratic interpolation, using independent interpolation for displacement and rotation, and cubic interpolation for displacement. The cubic elements are based on Euler-Bernoulli beam theory, which means that any transverse shear deformation is ignored. The linear and quadratic elements use Timoshenko beam theory and include shear deformation. A problem with the Timoshenko beam elements is that they tend to *shear lock* when the ratio between section depth and element length becomes smaller. This is because the shear term dominates the stiffness contribution as the beam becomes thinner. The problem can be eliminated using reduced integration. Only reduced integration schemes are therefore available for Timoshenko elements.

In addition to the pure displacement formulated elements, hybrid versions of all these elements are also available. The hybrid elements are designed to deal with very slender situations: where the axial stiffness is very large compared to the bending stiffness. The axial force is treated as an independent unknown together with displacements, resulting in a mixed formulation.

3.1.2 Modelling of contact

ABAQUS (Version 4.6) provides four basic types of interface elements for modelling contact between bodies. Gap elements may be used to model contact between discrete points, such as a pipe node and stinger roller. Interface elements are designed for contact over parts of surfaces where only small relative sliding between the surfaces may occur. The rigid surface elements are designed for the case where a deforming structure may contact a rigid body over part of its surface, and where large relative motions between these components may occur. A typical example is contact between a pipeline and the seabed. Slide line elements provide modelling for cases where two deformable bodies may make contact, and may undergo large relative motions such as contact between a flexible stinger and the pipeline.

In the direction of the normal between the surfaces, the surfaces may be considered *hard* or *softened*. The *softened* assumption models the presence of a local deformable layer on one of the surfaces in which case stiffness increases rapidly as the surface makes contact. The tangential surface traction may be defined by the assumption of dry friction.

3.1.3 Fluid environment

All the beam elements allow for loading associated with the immersion of the structure in a fluid. Fluid drag and inertia loading are provided by Morrison's equation. Buoyancy forces can also be included and is calculated depending on the orientation of the exposed surface area with respect to the vertical direction.

All the fluid-structure loadings require the definition of fluid density, free surface elevation, gravity constant, fluid particle velocities and accelerations. Fluid velocities are assumed to consist of two superposed effects: velocity caused by steady currents, (in which case velocity may vary with elevation), and velocity caused by gravity waves. Fluid accelerations are caused by gravity waves only.

Two types of wave theories, the linear Airy and Stokes 5th order theories, are available. Input data such as wave height, wave period and wave length define the response of the wave.

It is important to note that inclusion of a fluid results in a set of equations that are non-symmetric when written in matrix form. This is due to the nonlinear solution algorithm (Newton's method) which is employed by ABAQUS. In this method the Jacobian is created by taking variations of the difference between internal and external forces with respect to displacements. External forces are usually independent of displacements and the resulting Jacobian matrix is symmetric. Fluid forces are, however, nonlinear functions of velocity and acceleration, and their variations with respect to displacements result in a non-symmetric Jacobian matrix [28].

3.2 LOADING SPECIFICATION

The purpose of the analysis is to predict the response of the model to some form of external loading, or some non-equilibrium initial conditions. ABAQUS is based on the concept of analysis steps, each step being a portion or period of the history. For instance: the displaced shape of the pipe can be obtained in the first analysis or history step, and the dynamic response relative to the static profile in the second step. In nonlinear cases ABAQUS will increment and iterate as necessary to analyse a history step, depending on the severity of the nonlinearity.

3.2.1 Static analysis

Static analysis is used when inertia effects can be neglected: The analysis may be linear or nonlinear. ABAQUS uses Newton's method to solve nonlinear problems, with a quasi-Newton method as an alternative. The response is obtained as a series of increments, with iteration within the increment to obtain equilibrium. Equilibrium within an increment is obtained when all the residual stresses fall below a specified tolerance. These tolerances must be specified as a fraction of typical loads and reaction forces. The tighter the tolerance, the more accurate the results, but more computational effort is required.

The increment size is a matter of computational efficiency; if the increments are too large, more iteration will be required. Newton's method has a finite radius of convergence, which means that too large an increment can prevent any solution from being obtained because the calculated state is too far away from the equilibrium state which is being sought. Thus, there is an algorithmic restriction on the increment size. For this reason an automatic incrementation scheme, that selects the increment size based on the rate of convergence in previous increments, is available. In the case where the nonlinearity is not severe, and the user has experience with the particular problem, the direct incrementation scheme often provides a more economic solution. In this case a constant increment size is used.

3.2.2 Dynamic analysis

ABAQUS offers solution shemes for both linear and nonlinear dynamic response. Dynamic studies of linear problems are generally performed by using the eigenmodes of the system as a basis for calculating the response. Various response options are available: time history analysis, steady-state harmonic response and response spectrum analysis. It is important to note that Version 4.6 of ABAQUS does not have facilities to perform a probabilistic analysis, and the analysis must be performed in a deterministic way.

Direct integration for calculating the system's response must be used in nonlinear cases. Three methods are available: the Hilber-Hughes-Taylor operator, the central difference method and the subspace projection method. The Hilber-Hughes-Taylor operator is the most general method and was employed in this study.

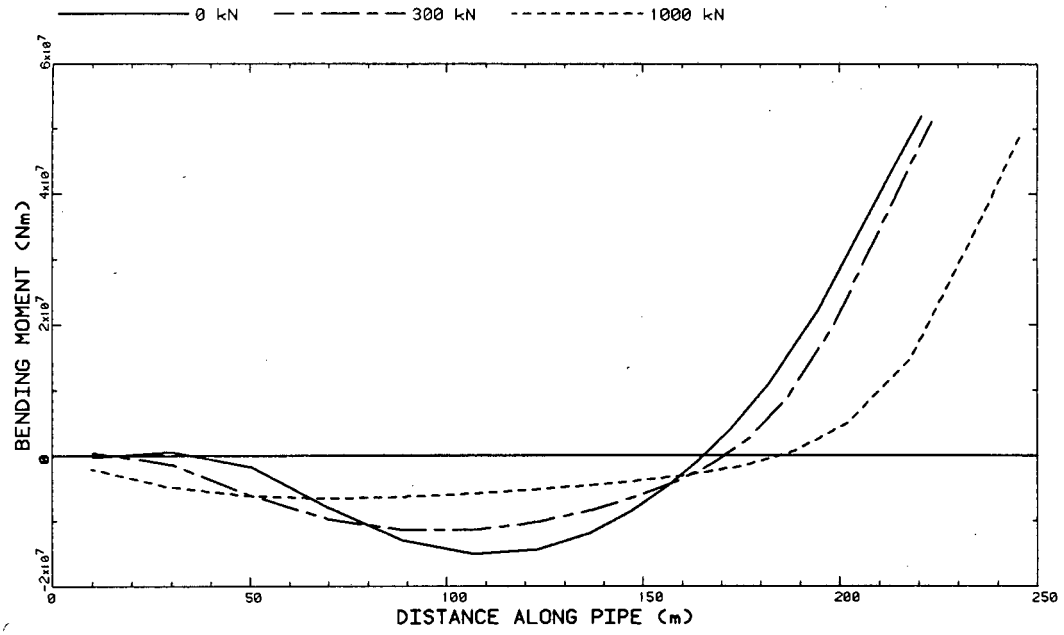

Figure 4.4: Bending Moments for Different Axial Forces

4.2.2 Seabed Studies

The objectives of this study were to determine the behaviour of the pipe in the region where it lies upon the seabed, and to determine the effect of a flexible seabed on the pipeline. To simplify the model the assumption was made that the barge tension reduces sagbend moments and the stinger support overbend moments. The stinger can therefore be omitted in this study, since it will have a negligible effect at the area of interest and will complicate the model unnecessarily. This assumption will be shown to be acceptable in Section 4.2.3.

Three different models were used to model the seabed. In the first model the seabed was presented as a *rigid surface*, in the second as a *beam on an elastic foundation*, and in the third as a set of *springs*. The purpose of the second and third models was to model a non-rigid seabed rather than a rigid seabed. In all the models the contact area was highly discretized.

The *rigid surface* model was exactly the same as the model described in the previous section. In addition different pressure-clearance relations (Fig. 4.5.) were used. The default relationship allows the body to be either in contact

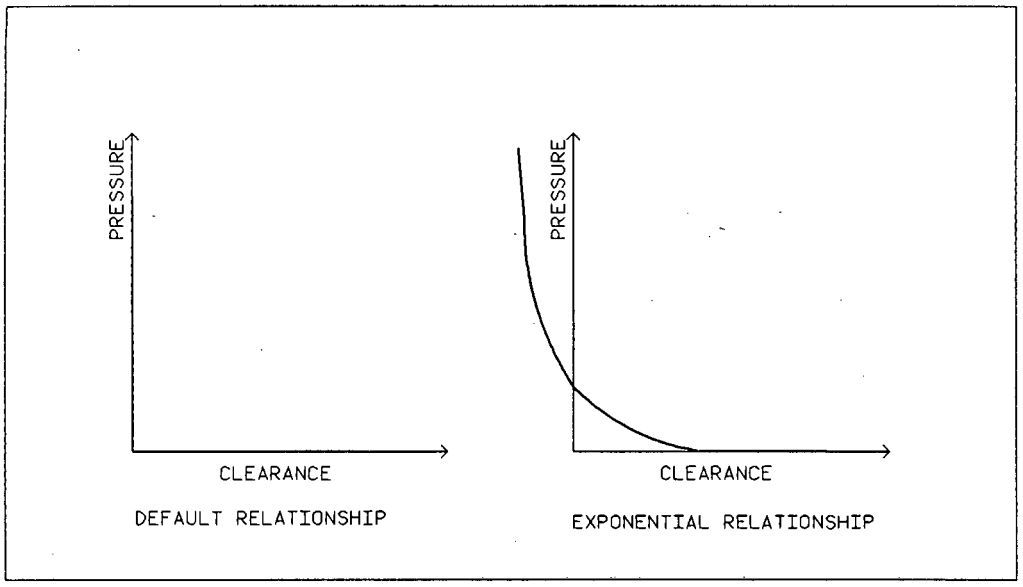

Figure 4.5: Pressure-Clearance Relationships

(zero clearance) or not in contact (zero pressure). Alternatively, an exponential relationship can be defined. This is a more accurate model of the physical situation, and it can also help numerically by adding some smoothing to a rather severe, sudden effect.

In the second model the seabed consists of a *beam on an elastic foundation* instead of the *rigid surface*. Contact between the pipe and the beam was established by the slide line elements. The stiffness matrix of a beam on an elastic foundation consists of terms due to the beam stiffness and terms due to the elastic foundation. A negligible beam size was used to obtain foundation stiffnesses only. The foundation stiffness must be defined in both the vertical and horizontal directions for the following reason:

The beam stiffness matrix is given as:

$$\mathbf{K}^e = \begin{bmatrix} k^e_{11} & 0 & 0 \\ 0 & k^e_{22} & k^e_{23} \\ 0 & k^e_{32} & k^e_{33} \end{bmatrix} \begin{matrix} u \\ v \\ \theta \end{matrix}$$

where the associated degrees of freedom are shown next to the stiffness matrix. The foundation stiffness in the vertical direction is given as:

$$\mathbf{K}^{f_y} = \begin{bmatrix} k_{22}^{f_y} & k_{23}^{f_y} \\ k_{32}^{f_y} & k_{33}^{f_y} \end{bmatrix} \begin{matrix} v \\ \theta \end{matrix}$$

and in the horizontal direction as:

$$\mathbf{K}^{f_x} = \begin{bmatrix} k_{11}^{f_x} & k_{13}^{f_x} \\ k_{31}^{f_x} & k_{33}^{f_x} \end{bmatrix} \begin{matrix} u \\ \theta \end{matrix}$$

If only the vertical foundation stiffness is chosen, the following situation arises after summation of the beam stiffness and foundation stiffness matrix:

$$\begin{aligned} \mathbf{K} &= \mathbf{K}^e + \mathbf{K}^{f_y} \\ &\approx \begin{bmatrix} 0 & 0 & 0 \\ 0 & k_{22}^{f_y} & k_{23}^{f_y} \\ 0 & k_{32}^{f_y} & k_{33}^{f_y} \end{bmatrix} \begin{matrix} u \\ v \\ \theta \end{matrix} \end{aligned}$$

Round-off error causes a zero on the diagonal and a singularity is experienced when the global system matrix is solved. To overcome this problem the horizontal stiffnessess must also be added, hence:

$$\begin{aligned} \mathbf{K} &= \mathbf{K}^e + \mathbf{K}^{f_y} + \mathbf{K}^{f_x} \\ &\approx \begin{bmatrix} k_{11}^{f_x} & 0 & k_{13}^{f_x} \\ 0 & k_{22}^{f_y} & k_{23}^{f_y} \\ k_{31}^{f_x} & k_{32}^{f_y} & k_{33}^{f_x} + k_{33}^{f_y} \end{bmatrix} \begin{matrix} u \\ v \\ \theta \end{matrix} \end{aligned}$$

Alternatively the horizontal degrees of freedom can be eliminated by constraining deflection in that direction.

In the *spring* model (Fig. 4.6.) vertical springs were defined between nodes on the seabed. Gap elements were used between the pipe nodes and upper spring nodes to establish contact. The lower spring nodes were constrained against all movement, whilst the top ones were totally free to move.

The solid line in Figure 4.7 shows the pressure distribution along the seabed, obtained with the *rigid surface* model, where the default pressure-clearance relationship was used. The reasoning behind the high pressure peak in the first few meters after contact is that, that distance serves as support for the unsupported pipe. The drop in pressure to zero is the area where a *back curvature* or *lift off* at the seabed occurs. The rest of the graph shows a

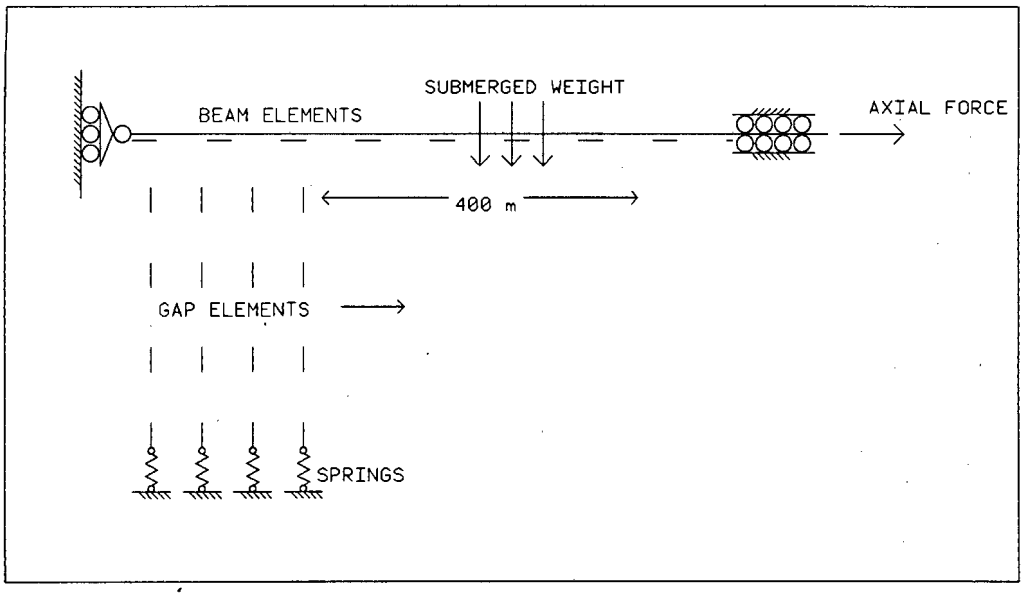

Figure 4.6: *Spring* Model

constant pressure which approaches the submerged weight (horizontal line) of 7460 N/m.

The dotted line in Figure 4.7 shows the pressure along the seabed where an exponential pressure-clearance relationship (Fig. 4.5) was used. The peak pressure obtained with an exponential relationship is lower but the total area under the curves (reaction force) remains the same. In this case the pressure does not drop to zero in the *lift off* area since there is a certain pressure associated with a small clearance. A better pressure distribution is obtained with the exponential pressure-clearance relationship, but a much longer runtime (62 % increase) was required.

Figure 4.8 compares the pressure distribution along the seabed obtained with the three different models. In all the cases the seabed was essentially rigid (for instance a stiffness of $k_f = 1 \times 10^{15}$ N/m was chosen for both the *beam on elastic foundation* and *spring* models). The same high peak is obtained with the different models. The *lift off* point in all the models was at the same point (viz. 83 m). The only difference is that the maximum peak pressure of the *rigid surface* model is lower than the pressure obtained with the *beam on an elastic founadtion* and *spring* models, but the reaction force (area under the curve) is still the same. In Figure 4.9 bending moments

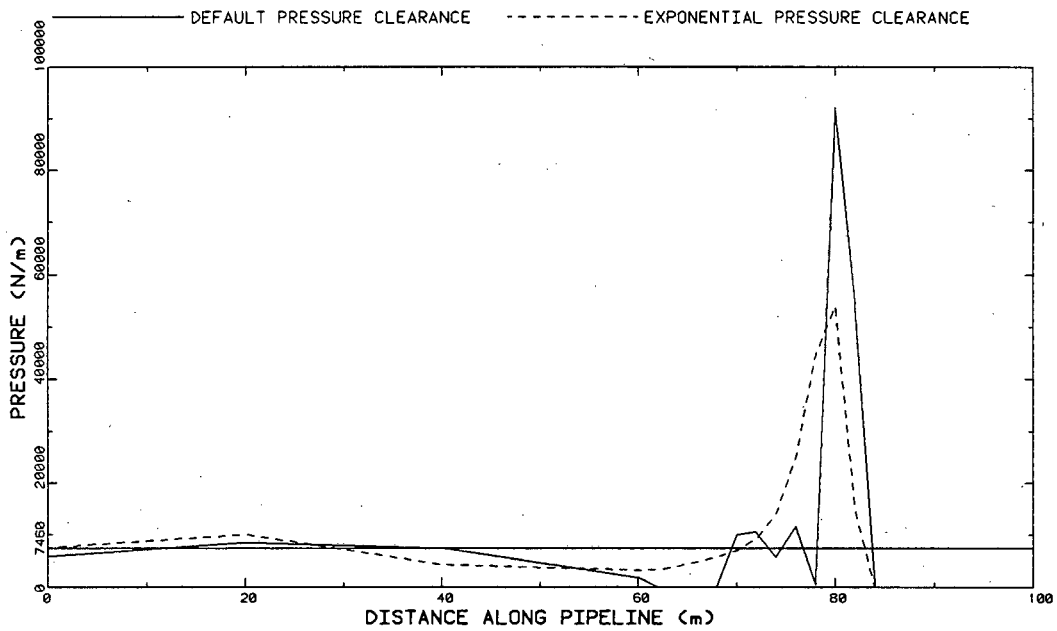

Figure 4.7: Pressure Distribution Along Seabed with different Pressure-Clearance Relationships

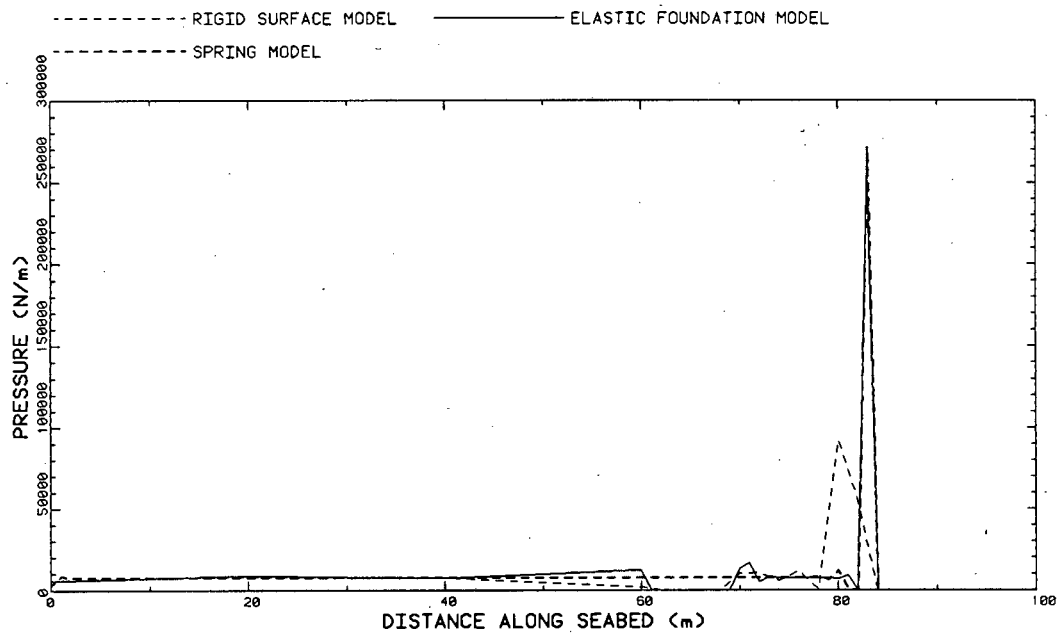

Figure 4.8: Pressure Distribution Along a Rigid Seabed Obtained with the Different Models

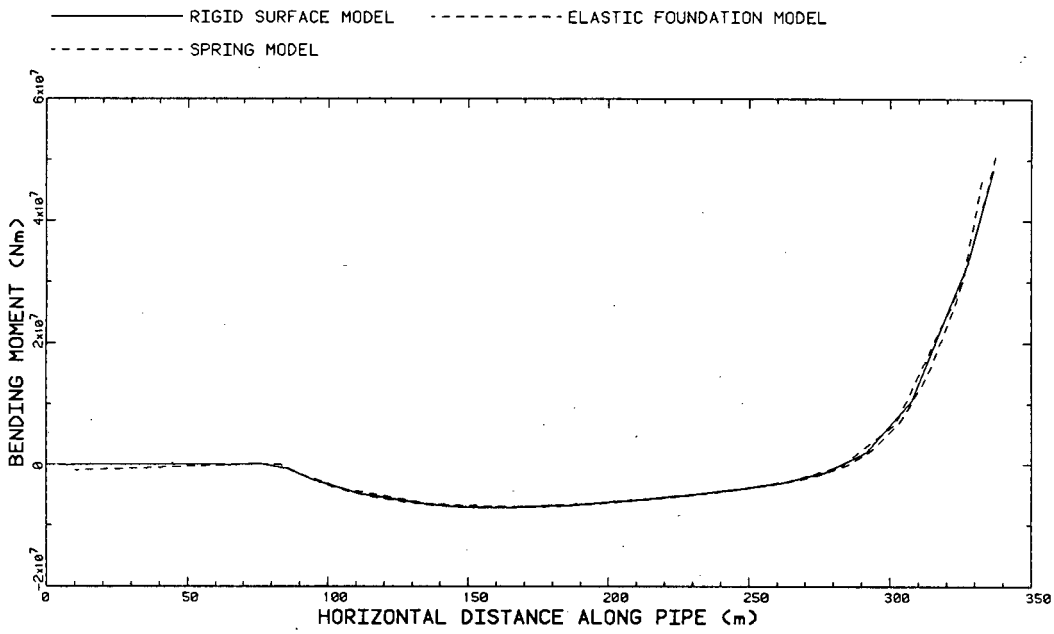

Figure 4.9: Bending Moments Along Pipe Obtained with the Different Models where a Rigid Seabed was used

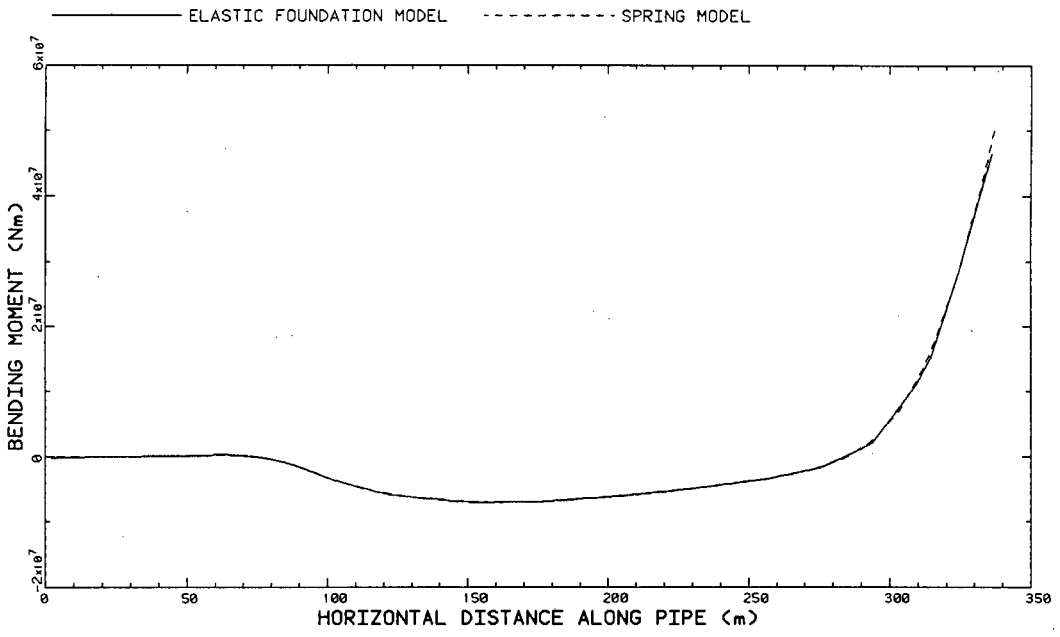

Figure 4.10: Bending Moments Obtained with Different Models where an Elastic Seabed was used

along the displaced pipe length is compared. Little difference exists between results obtained from the different models.

Figure 4.10 compares bending moment diagrams obtained from the *beam on elastic foundation* and *springs* models where an elastic seabed ($k_f = 100\ kN/m$) was used. Excellent agreement between the two models exists. The only difference lies in the practical application between the two models. The computation effort required in the *beam on an elastic foundation* model makes the model unattractive since the slide line elements used to establish the contact between the pipe and seabed are 6 to 8 times more expensive than other methods. Instead of slide line elements, gap elements can also be used to establish the contact. The feasibility of such a method was not tested in this study.

Figure 4.11 compares the pressure distribution along the seabed obtained with a rigid and elastic seabed. The *lift off* point for an elastic seabed has moved from 83 m to 98 m along the pipe, and the pressure distribution is now without the sharp peak. Figure 4.12 shows the difference between

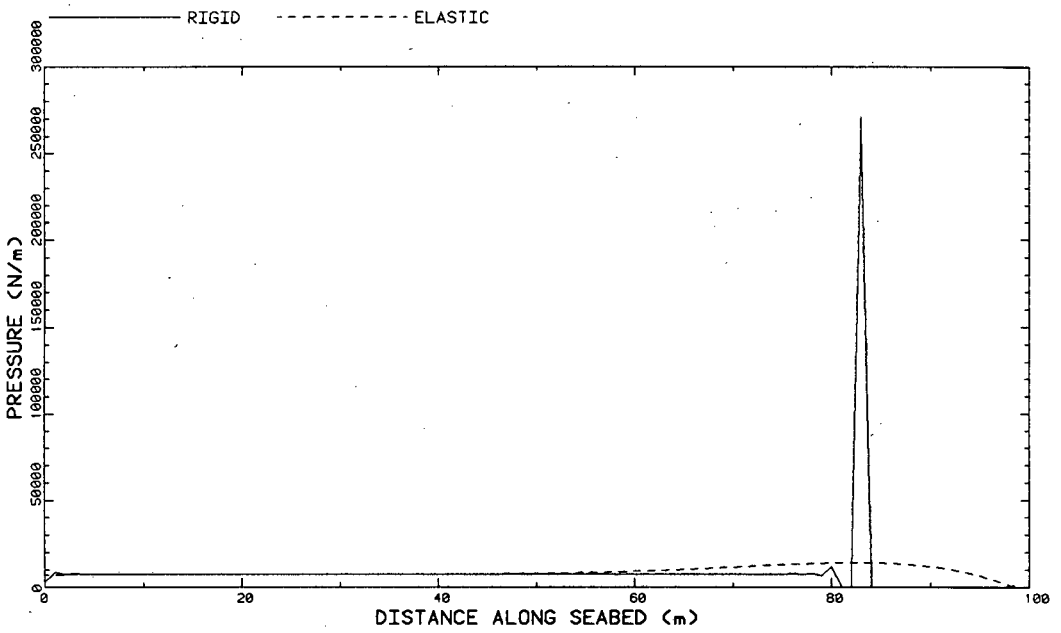

Figure 4.11: Pressure Distribution Difference between a Rigid and Elastic Seabed

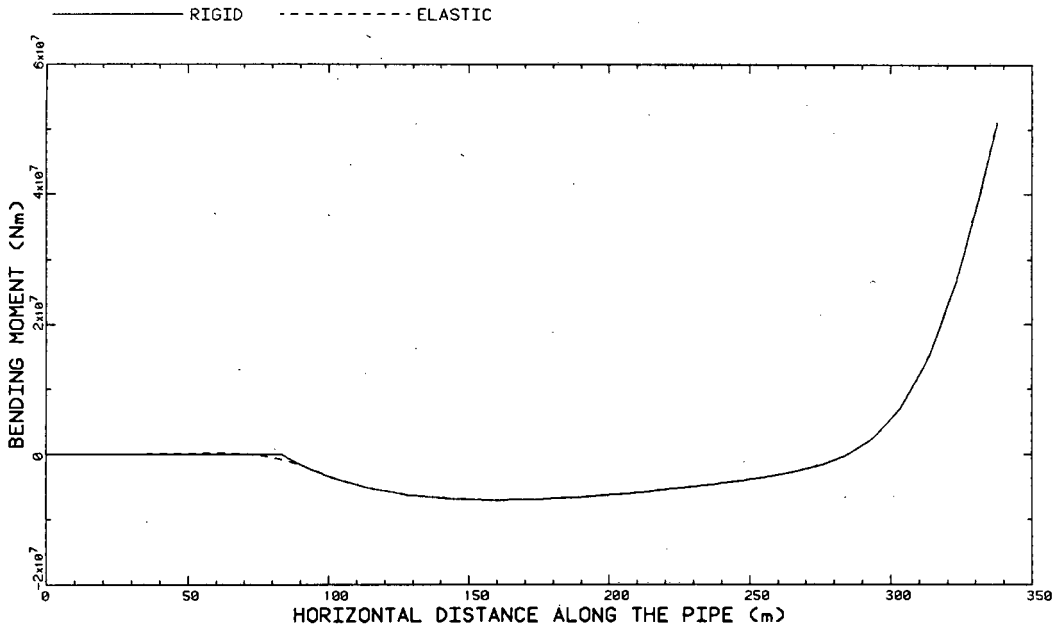

Figure 4.12: Bending Moments Difference along Pipe between a Rigid and Elastic Seabed

bending moments. Although a significant difference exist between pressure distributions at the seabed, the difference in global stiffness is negligible.

The seabed area has been modelled successfully. Whether the seabed is modelled as rigid or elastic, there is little difference in global pipe stresses. This is however, not necessarily the case for dynamic stresses.

One can therefore conclude, that the *rigid surface* model is sufficient to represent the seabed. If a flexible seabed has to be modelled either the *spring* model or the *beam on an elastic foundation* model can be used. Preference is given to the *spring* model to represent the flexible seabed since the *beam on an elastic foundation* model is more complicated to generate.

4.2.3 Stinger Studies

The stinger is an important part of the total system as it supports the pipe in the area where the high overbend bending moments occur. The articulated stinger, which consists of hinged elements, each one with its own buoyancy

pontoon, was modelled in this study. The shape of the pipe can be altered by changing the buoyancy of the different elements, and by a suitable combination of pipe tension and stinger shape, pipe stresses can be kept within prescribed limits for specific sea conditions. The stinger is a complex structure on its own, and it is not feasible to model it as such. Its interaction with the pipeline can, however, be modelled. As stated in Section 2.1 the stinger can be seen as exerting concentrated loads perpendicular to the pipe curve at the roller locations.

The objective with the stinger studies was to include the interaction of the pipe and stinger in the model. Two stinger models were developed initially. In these models the stinger was seen as something physical: the first model used a rigid surface and the second beam elements. They will be referred to as the *rigid surface* and the *beam element* models respectively. An important question, the effect of a flexible stinger will also be addressed.

Problems encountered with these models in the dynamic analysis led to the development of a third model where, instead of a physical stinger representation, concentrated forces were applied on the pipeline at the roller locations.

The *rigid surface* stinger (Fig. 4.13) was modelled as a continuous circular arch segment of 80 m length and 160 m radius, with contact established by rigid surface interface elements. In the *beam elements* model (Fig. 4.14), the beam nodes were defined at equal distances of 10 m along the stinger curve to represent 8 rollers. Gap elements were used between the pipe nodes and stinger nodes to establish contact. Only the stinger part of both models are shown in Figures 4.13 and 4.14 as the rest of the model was the same as the rigid surface seabed model described in the previous section.

An important feature of the problem is the unknown suspended length of the pipeline at the beginning of the analysis. In the modelling techniques adopted in this study, this phenomenon is manifested by the barge end of the pipeline that is allowed to move in a horizontal direction until equilibrium is reached. This makes definition of the stinger location difficult as the exact position is only known at the end of the analysis. A way to overcome this is to define the stinger at the undisplaced position of the pipeline at the barge end, and let the stinger move with the pipeline in a horizontal direction to the unknown position. This can be done with constraint equations. In the *rigid surface* model, the horizontal degree of freedom of the last pipe node and the rigid surface reference node were matched to be identical. In the *beam element* model the horizontal motion of the last beam node must be matched

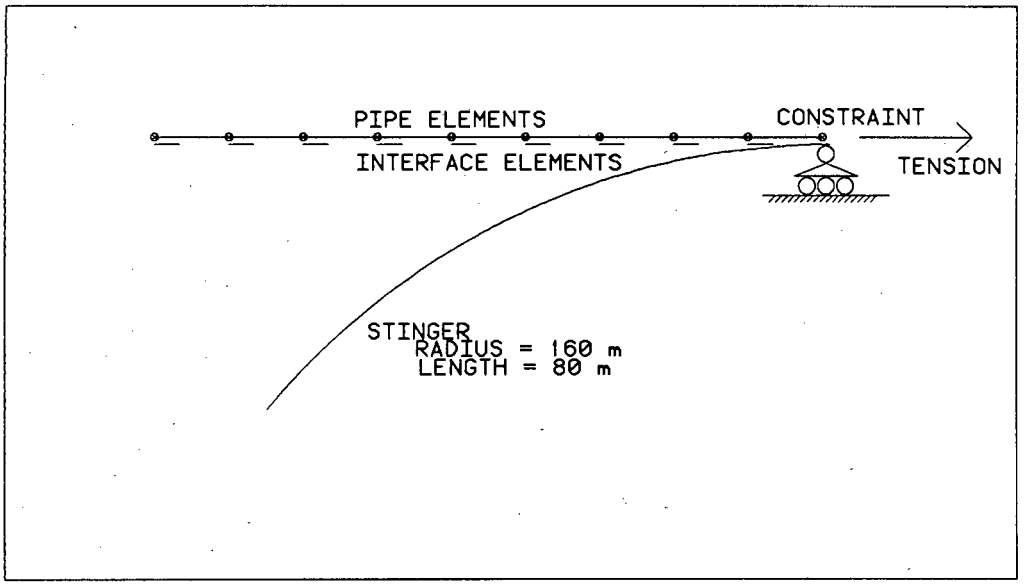

Figure 4.13: *Rigid Surface* Stinger Model

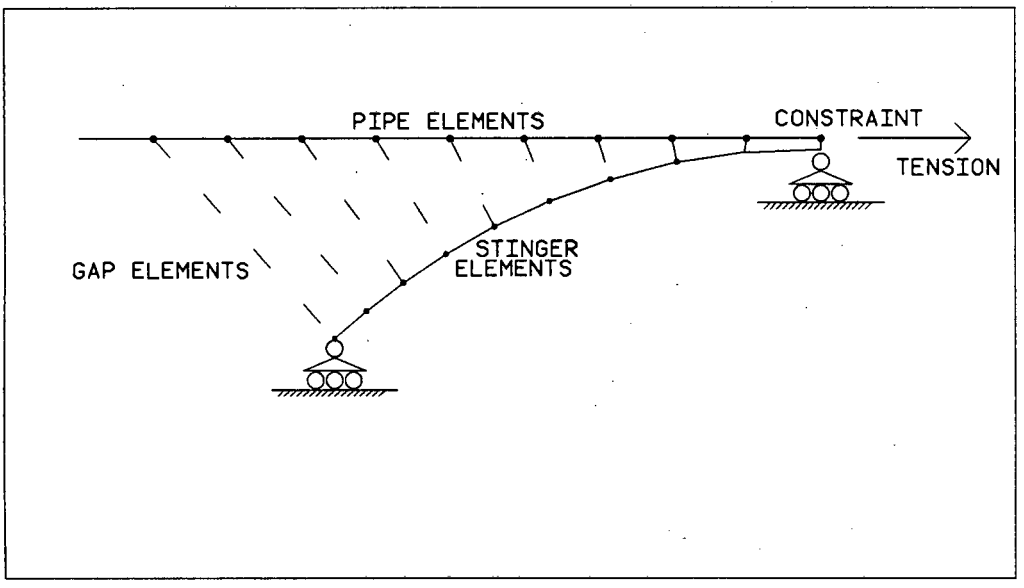

Figure 4.14: *Beam Elements* Stinger Model

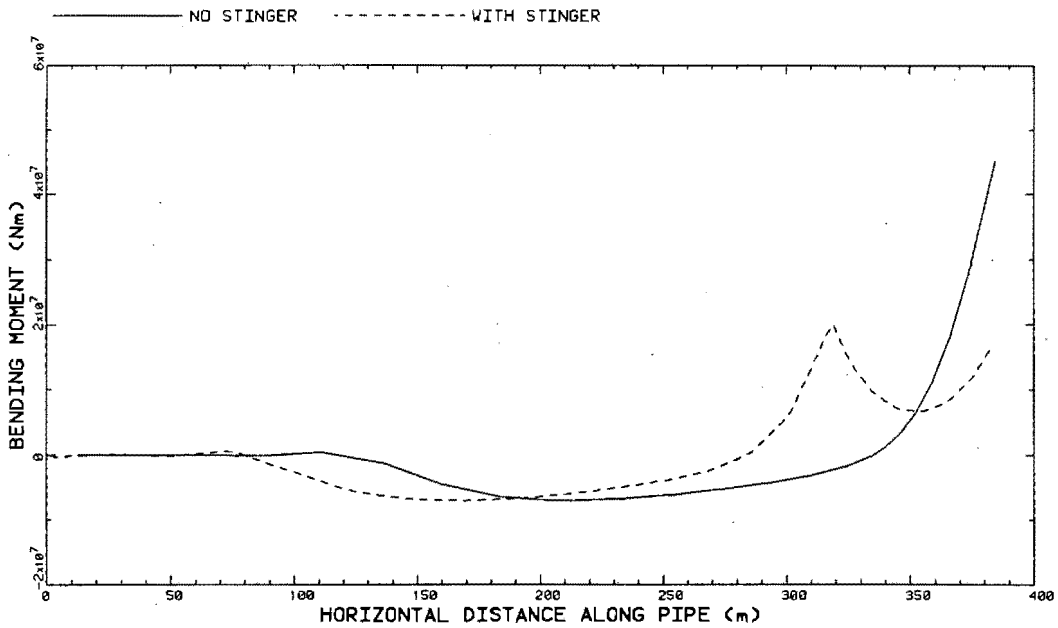

Figure 4.15: Bending Moments Along the Displaced Pipelength Otained with, and without the Inclusion of a Stinger

with the last pipe node. All the other degrees of freedom of the stinger (vertical and horizontal) must then be constrained against any movement.

Figure 4.15 shows the reduction in bending moment in the overbend region if a stinger is included. The location of the maximum sagbend moment has moved, but its value did not change significantly (less than 1 %). The maximum overbend bending moment is reduced by a significant 61 %. The assumption made in Section 4.2.2, that barge tension reduces sagbend moments and the stinger support the overbend moments, was therefore justified.

The reason for the sharp bending moment peak in the overbend region is caused by a very high reaction force at that location. The chosen stinger geometry was unfortunately such that contact was not established at all the roller locations resulting in high reaction forces at some, and no reactions at other rollers. The ideal stinger geometry is one that supports the pipe so that each roller exerts the same reaction force on the pipeline.

Bending moments obtained with the *rigid surface* and *beam element* stinger models are compared in Figure 4.16. Small differences exist in the stinger

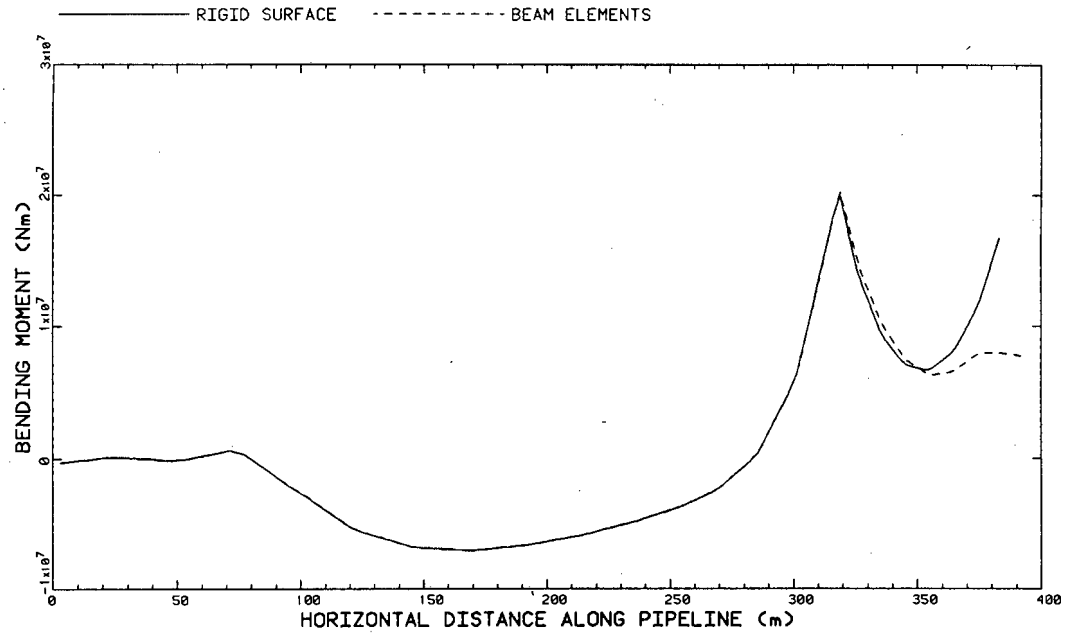

Figure 4.16: Bending Moments Along Pipe Obtained with Different Stinger Models

region only. This is because the rigid surface elements provides continuous contact, whilst gap elements provide contact between discrete points only.

In both models discussed, the stinger was modelled as being rigid. It is however important to investigate the effect of stinger flexibility on the pipeline. This can be accomplished by releasing the vertical and rotational degrees of freedom at all the stinger nodes (Fig. 4.14.) except at the last node at the barge end. The problem is to find a typical stinger stiffness value, as this data is not readily available in literature.

To simulate a displaced stinger, a model was created whereby the circular stinger arc was rotated at the barge end in such a way that the tip was displaced by approximately 5 m. Bending moments obtained from the *displaced* and *undisplaced* stinger models are compared in Figure 4.17. The values of maximum and minimum moments did not change significantly although their location moved. For instance, the maximum overbend bending moment moved from 319 m to 327 m.

The conclusion is that stinger flexibility alters the pipe shape and therefore

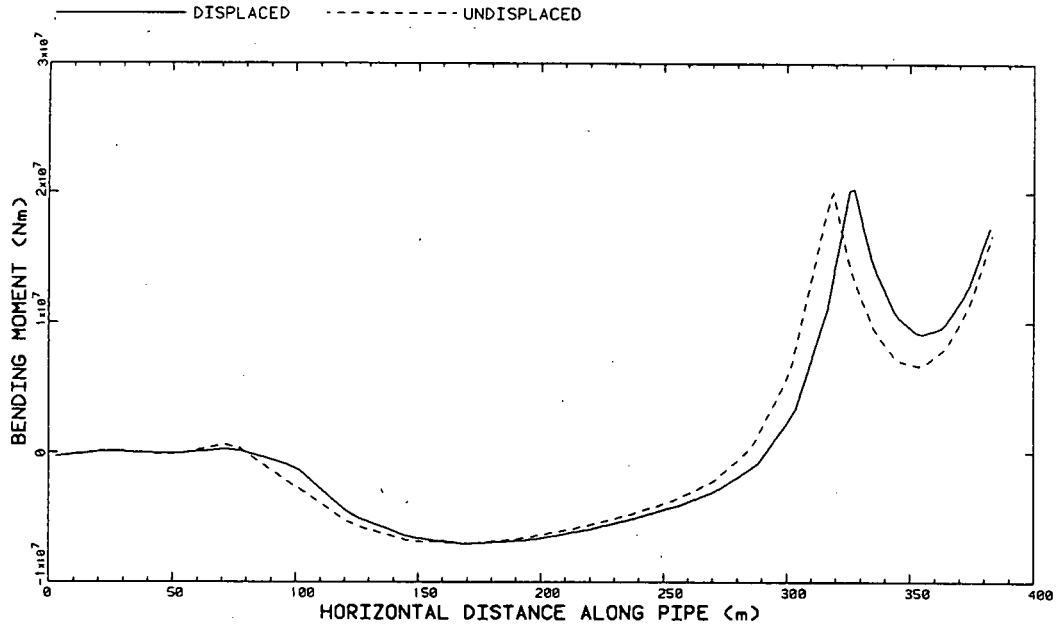

Figure 4.17: Bending Moments Along Pipe Obtained with a Displaced and Undisplaced Stinger

the location of the peak moment, but does not change the value significantly, and a rigid stinger representation is sufficient.

This conclusion can also be supported with the following argument: the position of the stinger can be altered by the barge operator by changing the buoyancy of individual element pontoons. If the stinger is flexible and displaces under pipe weight, the barge operator can change the stinger position back to the undisplaced position. The original position is restored, and the pipeline is *unaware* of stinger flexibility.

In order to find a stinger geometry where each roller carries a uniform reaction, the *equivalent force* model was used. To test the feasibility of the method, the reaction forces obtained from the *beam elements* stinger model were applied on the pipe at the roller locations. Bending moments obtained with the two methods are compared in Figure 4.18. The slight discrepancy between bending moments is due to the fact that the equivalent forces were applied vertically rather than perpendicular to the pipe curve.

Another source of error is the way in which these forces are applied. It is

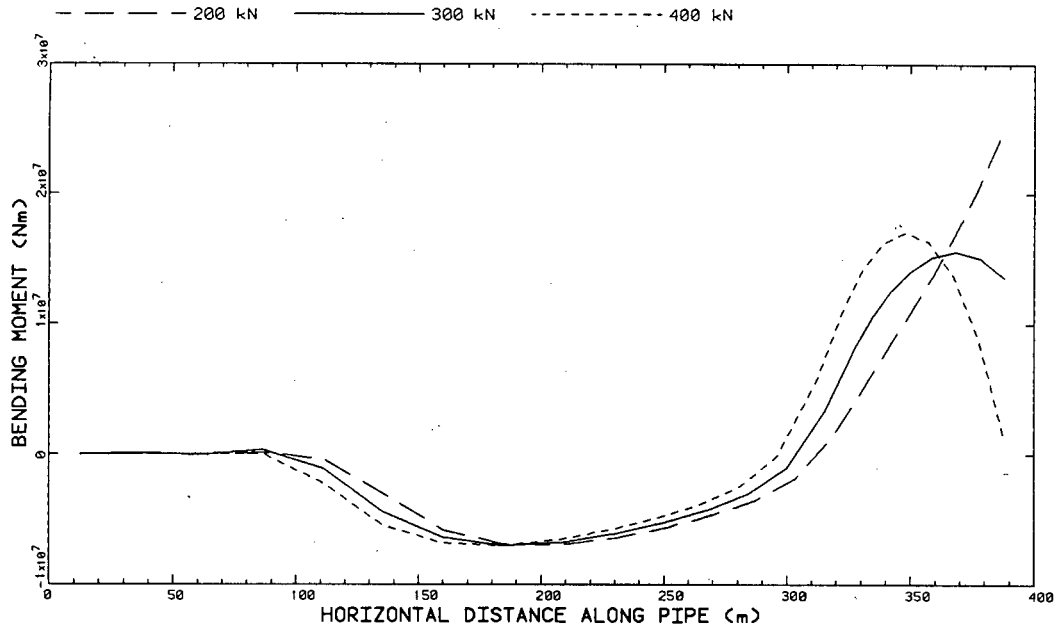

Figure 4.19: Bending Moments Along Pipe Obtained with Uniform Concentrated Loads

important to apply these forces after an initial displaced curve is obtained, rather than in the beginning of the analysis. In fact, the results are completely incompatible if these forces are applied in the beginning of the analysis. The reason behind this is that the applied forces are a function of geometry, $\mathbf{K}(x)\mathbf{x} = \mathbf{F}(x)$, in the nonlinear case and the global stiffness matrix is updated (according to these loads) after each load increment is taken. If the equivalent forces are applied in a second step, after an initial curve is obtained and the structure is stiffened, they affect the geometry not as severely as in the case when they are applied in the beginning of the analysis.

Figure 4.19 shows bending moments obtained with different uniform concentrated loads. A much smoother curve is now obtained. Pipe stresses obtained using 300 kN loads at the different roller locations result in the optimum situation.

The choice between the models lie in the feasibility. The *beam elements* stinger is preferred above the *rigid surface* stinger because it implies the

discrete interaction at the stinger rollers only. The disadvantage is that the direction of the gap between a pipe node and corresponding stinger node must be calculated for each pair as they differ in general. This results in a different gap element specification for each node pair, and the gap option must be defined for all the pairs independently. This can be time consuming and results in large data files to represent the stinger system. The advantage of the *equivalent forces* stinger above the *beam elements* stinger and *rigid surface* stinger is that the complexity due to contact is eliminated.

Other advantages and disadvantages of these models will be discussed in the next section.

4.3 DYNAMIC ANALYSIS

In the previous sections, only time independent loads were applied to the structure. This enabled development of the model under relatively simple loads. Time dependent loads are, however, of fundamental importance since they account for a significant fraction of the structural loading [8].

The objective of the dynamic study is not to give detailed information about dynamic pipe stresses, but to develop a suitable model which can provide the base for future study. The philosophy is to keep this model as simple as possible, but of sufficient complexity to adequately describe the areas of interest.

The approach followed is that of determining maximum stresses due to a series of harmonic waves and barge motions (which act on the structure during a relatively short time history; eg. in the order of 2 or 4 wave periods) in a deterministic way. However, if observations of these motions are made over a longer time period, it is apparent that their properties vary randomly with time. The most convenient way to account for random events is to use the linear probabilistic analysis in the frequency domain, where the random loads and response of the structure can be expressed by means of spectral density curves. Since probabilistic analysis is not available in Version 4.6 of ABAQUS, no random vibration nor statistical analysis has been attempted in this study.

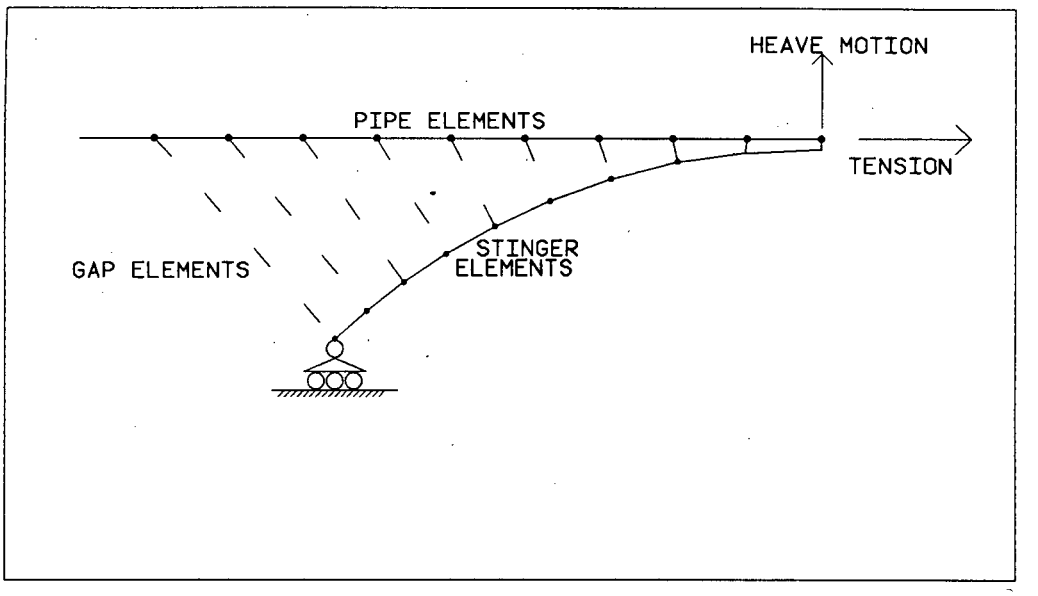

Figure 4.20: *Beam Element* Stinger Model for Dynamic Excitation

4.3.1 The Finite Element Models

Several models have been used. In all these models the seabed was modelled as a rigid surface. The limitations in all the models are mainly imposed by the way the stinger is represented, and whether fluid properties are specified or not. Limitations imposed by a fluid will become apparent in the next section.

The *rigid surface* stinger model described in Section 4.2.3 is impractical in dynamic analysis since only one reference node exists which can be excited with the heave motion. This means that the whole stinger will follow the motion of this reference node, which is not what happens in the practical case where motion towards the end is damped out due to fluid-structure interaction.

The *beam element* stinger model is more practical since the two ends of the stinger can be excited independently (with a small motion at the stinger tip and a bigger motion at the barge end) to represent the assumed stinger motion. Figure 4.20 shows the boundary conditions for this model: the barge end is excited with the heave motion whilst the tip is restrained against vertical motion but can rotate and move in a horizontal direction. Motion

in these directions must be permitted, otherwise the stinger will be stressed by the barge tension. This is undesirable since only the pipe is stressed by the barge tension in the practical case.

A cheap solution can also be obtained with the use of the *equivalent forces* stinger model since complexities due to contact are eliminated. The assumption in this case is that there is no contact or lift-off between the stinger and the pipe, but continuous contact with constant reactions at the roller locations.

4.3.2 Nonlinear Time Domain Analysis

This section discusses results obtained from a nonlinear dynamic analysis. Large displacements relative to the static profile and contact of the pipe at the seabed and stinger are allowed, and nonlinear hydrodynamic forces are applied. An implicit integration scheme (see Section 3.2.2) was used to obtain the response of the structure.

It was observed that a steady state condition is usually reached after 2 to 3 cycles and the response of the structure was therefore determined over a dynamic time period of 40 *sec.* ($\approx$ 3 cycles).

Figure 4.21 shows a bending moment envelope obtained with the *beam elements* stinger model where the pipe was excited with barge motions only. To compare the *equivalent forces* and *beam elements* stinger models, the reaction forces obtained from the *beam elements* stinger model were applied at the roller positions of the *equivalent forces* stinger model. A comparison between the two methods (Fig. 4.22 and 4.21) shows that conservative results can be expected from the *equivalent forces* stinger representation.

As mentioned in Section 4.2.3, the stinger geometry chosen for the *beam elements* stinger model was such that contact was not established at all the rollers, resulting in large reactions at some rollers, and no reaction at others. A stinger that supports the pipe in such a way that each roller exerts approximately the same force, will result in the optimum situation. It has been shown in Section 4.2.3 that the high peak at the stinger tip can be eliminated, and that the bending moments are least when 300 kN uniform forces are applied at the roller locations. Figure 4.23 shows a bending moment envelope when this model was excited with barge motions only. It is apparent that not only do the static moments decrease, but there is also a reduction in dynamic moments.

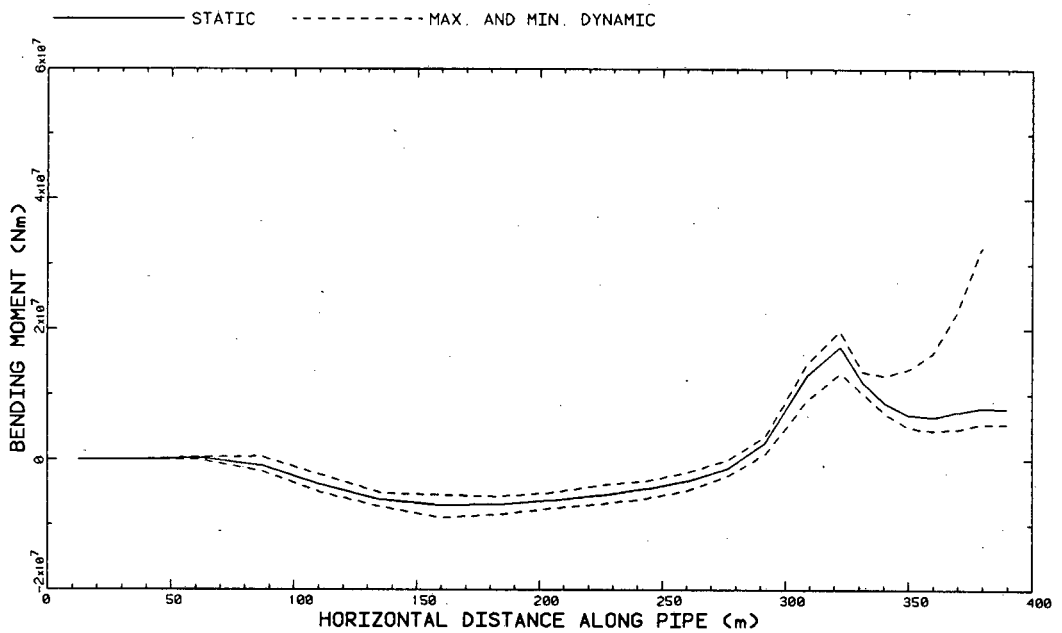

Figure 4.21: Bending Moment Envelope Obtained with *Beam Elements* Stinger Model

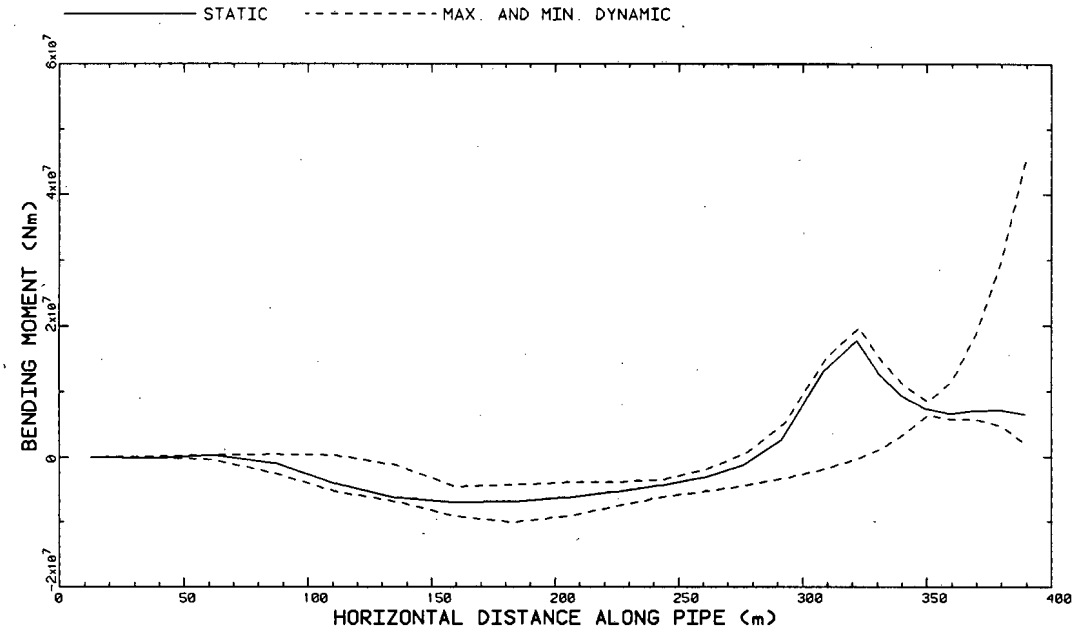

Figure 4.22: Bending Moment Envelope Obtained with the *Equivalent Forces* Model

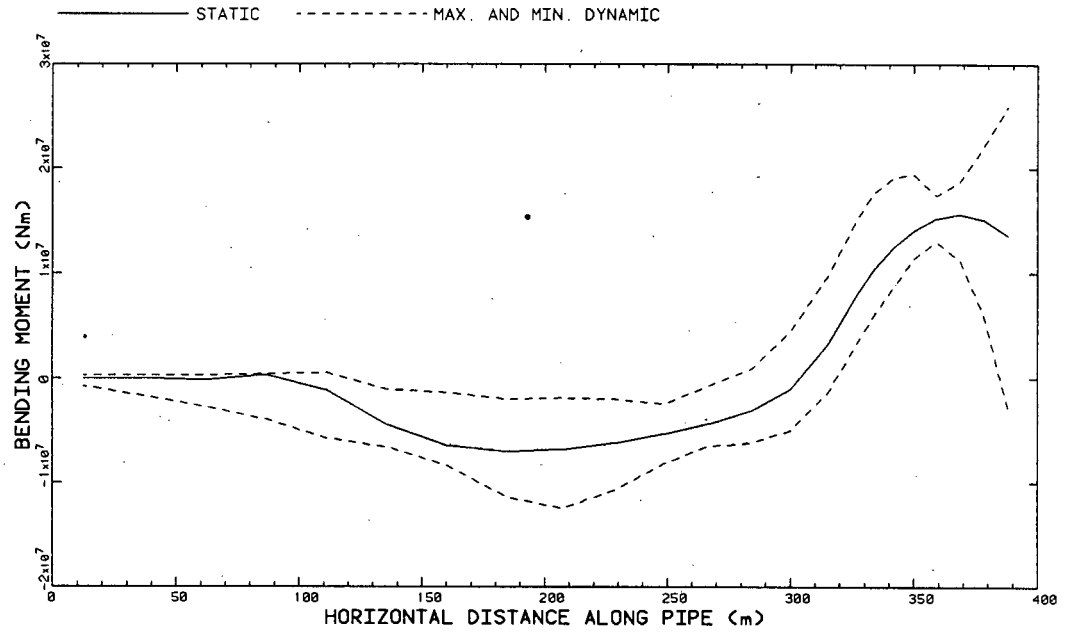

Figure 4.23: Bending Moment Envelope Obtained Using Uniform 300 kN Equivalent Forces

The effect of drag and inertia forces on the structure has been discussed in Section 2.1.3. These forces result from relative motion between the structure and fluid, and must be accounted for in the dynamic analysis. The inclusion of these forces introduces numerous solution problems. For instance: no results could be obtained when a fluid was specified in the presence of gap elements. In addition, only linear displacement formulated elements could yield results. No reason for this could be found, but it might be due to a bug in the code.

Alternatively, contact can also be established with the slide line elements. The use of the slide line elements is unfortunately extremely expensive. It can take up to 8 times as long to obtain a solution as compared to an alternative method.

The use of an *equivalent forces* stinger model eliminates complexities due to gap elements, and a cheap solution is therefore possible. In the rest of the discussion, the stinger was approximated with uniform 300 kN loads applied at the roller locations. Figure 4.24 shows a bending moment envelope obtained where drag and inertia effects are included, but where forces calculated by Morison's equation are due to structural motion only (eg. no waves or currents are included). A drag coefficient of 0.7 and inertia coefficient of 1.0 were used which are typical values used in offshore analysis. Comparison with Figure 4.23 shows how the drag forces damp out motion.

To determine whether velocities and accelerations resulting from waves introduce significant forces on the pipe, a wave (based on Stokes theory) was included. A comparison between bending moments for this model (Fig 4.25), and a model without any waves (Fig. 4.24), show only a 2.8 % increase in the maximum bending moment, and the conclusion is that barge motions account for most of the dynamic loading.

In preceeding discussion, the seabed was assumed to be a rigid surface. It is, however, important to investigate the effect of a flexible seabed on pipe stresses. A flexible seabed can be modelled by either using individual spring elements, or a beam on an elastic foundation, with contact being established by gap elements. As mentioned before, gap elements do not work in the dynamic case when the structure is immersed in a fluid. This limits the analyst to model the presence of a flexible seabed in air only. Bending moments obtained from such an analysis are shown in Figure 4.26. A comparison with bending moments obtained from an analysis with a rigid seabed (Fig. 4.23), show that the maximum bending moments do not differ significantly, and a

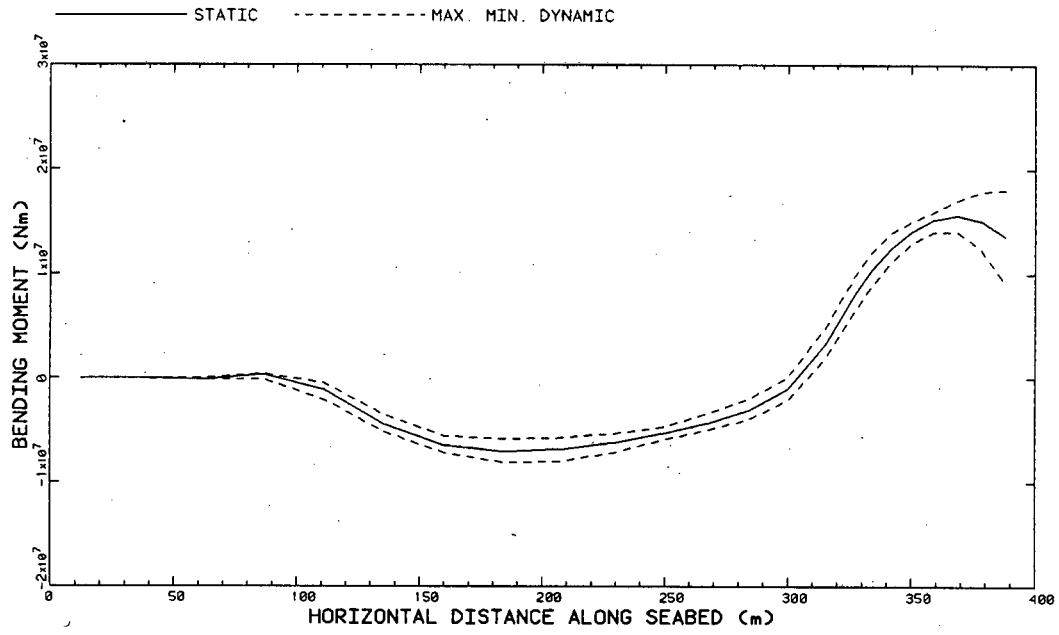

Figure 4.24: Bending Moment Envelope with Drag and Inertia Effects Included

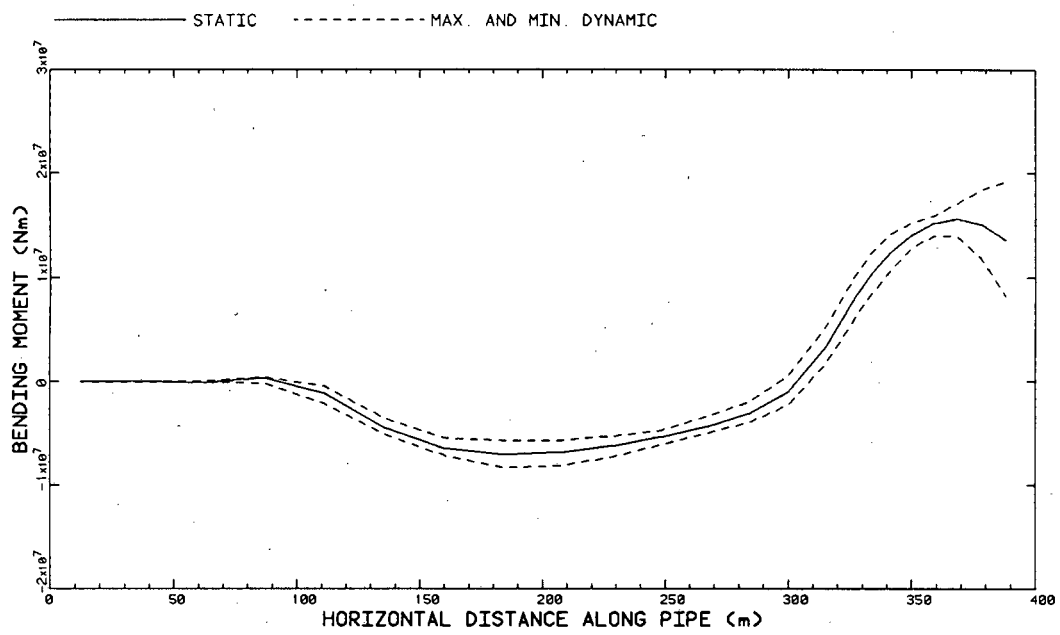

Figure 4.25: Bending Moment Envelope were a Stokes Gravity Wave was Included

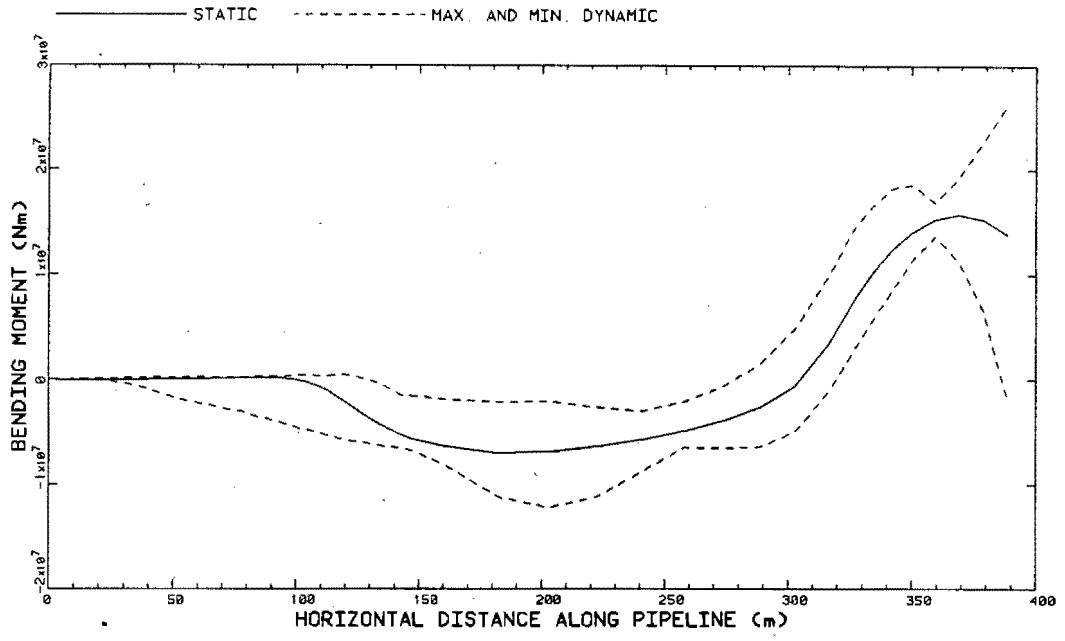

Figure 4.26: Influence of a Flexible Seabed on Bending Stresses

rigid representation is sufficient.

Table 4.1 summarises the results obtained in the nonlinear dynamic studies.

Analysis	Max. Sagbend Moment	Max. Overbend Moment
	Ratio of Dynamic versus Static Moment	
No Fluid	1.77	1.67
Fluid Included	1.15	1.16
Wave included	1.18	1.23
Soft Seabed	1.74	1.69

Table 4.1: Summary of Dynamic Bending Moments

4.3.3 Excitation Near the First Natural Frequency

If a structure is excited near the frequency of one of its mode shapes, resonance, with a result in high stresses, will occur. The natural frequency of a structure is a function of the mass, stiffness and damping of the structure. The following relationship exists for a single degree of freedom system:

$$\omega = \frac{1}{2\pi}\sqrt{\frac{K}{M}(1-2\xi)} \tag{4.1}$$

where:

ω = Natural Frequency
K = Stiffness
M = Mass
ξ = Damping Ratio

It is apparent that the natural frequency of a structure immersed in a fluid will differ from one in air. For instance: the stiffness of a structure in water is reduced by the buoyancy force in a nonlinear problem, the mass is increased by the added mass effect, and the damping ratio is increased by drag. This means that the natural frequencies of a structure in water will be much lower than the frequencies of the same structure in air.

It is, however, impossible to extract the natural frequencies of a structure surrounded by a fluid using Version 4.6 of ABAQUS. Specification of fluid properties invokes a non-symmetric system matrix, whilst the subspace iteration method, which is used to extract the natural frequencies, assumes a symmetric stiffness matrix (see Sections 3.1.3 and 3.2.2). A way to overcome this problem is to extract these frequencies in the absence of the fluid by using alternative methods to account for the effects of buoyancy, added mass and drag.

An equivalent submerged weight can be applied instead of self weight and buoyancy. The added mass is usually assumed to be equal to the mass of water replaced by the structure, multiplied by the inertia coefficient [26] [8]. The additional mass calculated this way can simply be lumped at the pipe nodes. Drag can be neglected since it will not change the natural frequency significantly, but will merely suppress motion at resonance. Table 4.2 gives the natural frequencies of the first four mode shapes obtained using the procedure outlined above. In addition, the corresponding frequencies when

Mode Number	Added Mass Included		Without Added Mass	
	Freq. (rad/sec)	Period (sec)	Freq. (rad/sec)	Period (sec)
1	0.377	16.67	0.482	13.04
2	0.520	12.08	0.665	9.45
3	1.165	5.393	1.488	4.22
4	1.809	3.473	2.311	2.72

Table 4.2: Frequencies for Different Mode Shapes

no additional mass is lumped at the nodes, are also shown. It is apparent that only the first two mode shapes are of importance, since the higher mode shapes do not lie in the range of typical wave frequencies.

To verify whether resonance will occur at the fundamental frequency or whether drag will supress most of the motion, a number of analyses were done in the frequency range of typical wave and barge motions. These analyses were done without any of the abovementioned approximations, but a fluid was specified, and the effects due to drag, buoyancy and added mass were accounted for.

The solid line in Figure 4.27 shows the variation of bending moment at a typical element in the sagbend region with wave and barge motion frequency. The first observation is the two peaks which imply the first two natural frequencies. The first mode shape occured at a frequency of approximately 0.475 rad/sec and the second at a frequency of 0.650 rad/sec. A comparison with Table 4.2 shows that these frequencies correspond more closely to the frequencies obtained without additional mass lumped at the nodes. This means the added mass approximation (that the added mass effect is equal to the mass of the water displaced by the structure, multiplied by the inertia coefficient) is an overestimation. This is because the pipe is slender and therefore drag dominated, and the additional mass assumption applies to bigger inertia dominated members only.

If the dotted line is taken as the increase in bending moment with frequency in the absence of resonant effects, an estimation of the dynamic amplification at resonance can be obtained relative to this line. The amplification at the first natural frequency is approximately 6 % and 5 % at the second frequency. This is a relatively small amplification and is due to the damping effect of drag.

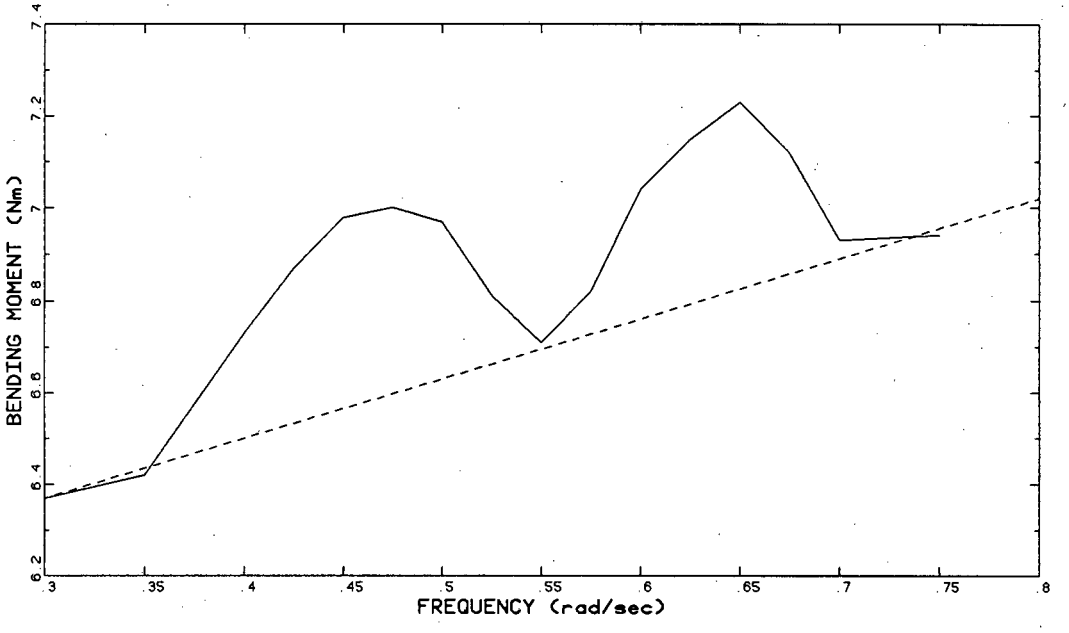

Figure 4.27: Effect of Wave Frequency on Maximum Sagbend Bending Moment

4.3.4 A linearized Dynamic Model

The pipelaying problem is characterised by nonlinear effects that increase the complexity. These effects include large displacements and rotations, contact at both the stinger and seabed, and the nonlinear drag force. Some of these nonlinearities can be linearized, and a linear dynamic or modal analysis rather than a nonlinear time domain analysis, can be performed.

The large displacements and rotations are usually neglected by assuming small dynamic response relative to the static displacements [25]. Contact at the seabed can be replaced by fixing the pipe nodes in contact with the seabed. Stinger contact can be ignored by assuming that the pipe stays in contact over the full stinger length. This means the bending moment at the stinger tip is known (since the stinger curvature is usually known) and can be applied as a boundary condition on the pipe at the free end of the stinger. The part of pipe in contact with the stinger, and the stinger, can now be neglected, and only the remaining part analysed [7] [46]. Alternatively, equivalent forces at the roller locations can simply be applied. The nonlinear drag force can be replaced with a linear part and an error function. The error function can then be minimized and ultimately neglected (Section 2.5).

In order to perform a linear dynamic analysis with the use of ABAQUS, a suitable model where all the linearized assumptions are incorporated, must be developed. Possible models and their limitations are discussed below.

The large displacements and contact can be eliminated by generating a new mesh using the restart option. The first step is to define the new model based on displacements obtained in the static analysis. The initial stresses and strains are mapped onto the new mesh, and after the pipe nodes in contact with the seabed are fixed, the contact elements are removed by using the element removal option. Although the complexities due to large displacements and contact are eliminated, implementation complexities are now introduced. The use of special features such as restart and element removal analysis are only recommended for the experienced analyst. Since a linearized model is only attractive when it is also easy to implement, an alternative method must be used.

Instead of using contact elements between the pipe and a physical seabed (such as a rigid surface), the pipe nodes that must contact the seabed can be displaced a vertical distance downwards corresponding to the sea depth. This can be done with a prescribed boundary condition. Once these nodes

have been displaced the required amount, they can be fixed, and a linear modal analysis relative to the static profile can be performed.

ABAQUS Version 4.6 offers application of a nonlinear drag force only, and since velocities and accelerations are not available for transfer between the main program and the user subroutine, linearization through the use of a user subroutine is not possible. An alternative is to neglect the presence of a fluid completely, and account for contributions from buoyancy, added inertia and drag by the assumptions discussed in the previous section. The limitation is that the drag term must then be neglected completely. Comparison of Figure 4.23 and Figure 4.24 shows that omission of the drag force effects the results considerably. Similar results have been obtained by Larsen [35]. The variation of maximum bending moment with different drag coefficients is also discussed in Section 5.1.3.

4.4 CONCLUSION

This chapter discussed various finite element models which can be used to model the pipelaying problem. The main areas which characterise the problem, such as geometric nonlinearity, contact of the pipeline at the seabed and stinger, and the fluid-structure interaction were included. The different models were compared, problems encountered and their causes were identified, and solutions were given.

Although some ideas received only cursory attention, these ideas and approaches can serve as a useful base for future study. For instance, a complete three-dimensional model can be developed and the response of the pipeline due to irregular wave action and barge motions can be studied.

5 GUIDELINES

The structural analyst usually has uncertainties regarding the finite element model such as, the level of discretisation, size of elements to use and the size of tolerances. Not only does the accuracy of the results depend on proper selection of these parameters, but the performance can be increased considerably.

This chapter attempts to assist the user in selecting a proper model which will yield reliable results relatively quickly. Section 5.1 addresses details about the model specification, whilst the loading specification is discussed in Section 5.2.

5.1 MODEL SPECIFICATION

5.1.1 The Finite Element Model

Two distinct methods of analysis are available to the analyst: the pipe can be defined in the unstressed state on either the seabed or sea surface. If the model is defined on the seabed, the barge end must be displaced to the seabed in the analysis or history step. The second method, where the pipe is defined on the surface and then allowed to drop to the seabed, was used in this study.

The seabed can be modelled in various ways depending on what is required from the analysis. The simplest case is to model a rigid seabed. This can be accomplished with the use of the rigid surface option or by defining fixed nodes on the seabed. If a flexible seabed is of interest, either springs between nodes or a beam on an elastic foundation, can be used. It was however found that gap elements, which are required to establish contact, do not work when associated with a fluid in a dynamic case using ABAQUS Version 4.6. Slide line elements can be used instead of gap elements, but their use is not recommended since they are very expensive.

The stinger can also be modelled with a rigid surface. The only limitation is that only one node can be defined on the rigid surface. This means that the whole stinger will follow the motion of this reference node when it is excited with the barge motions. Instead of a rigid surface, the stinger can be made of beam elements, with gap elements between the pipe nodes and stinger

nodes to establish the contact. The limitation is again the combination of gap elements and a fluid in the dynamic case. Alternatively, equivalent forces at the roller locations (with the assumption that the pipe stays in contact, and the reaction force at the rollers are constant throughout the dynamic analysis) can be used.

5.1.2 Performance of the Different Elements

An important question is the level of discretization required and which of the available elements should be used in both the static and dynamic analysis. The suitability of an element will primarily be a function of the accuracy of the results and the computational effort needed to use the element. The codes used by ABAQUS for the different element types is also adopted here, and the theory, type of formulation, number of interpolation points and number of nodes for the different elements available, are given in Table 5.1.

Table 5.2 compares the performance of the different element types available. The maximum overbend bending moment obtained with a cubic interpolation scheme is about 17 % higher than the bending moment obtained with a linear interpolation scheme. This means that the stiffness calculated with cubic interpolation is smaller than that obtained with linear interpolation, and that linear interpolation therefore gives less conservative results. This is an important observation since the linear interpolation scheme is much cheaper than cubic interpolation.

Another observation from Table 5.2 is the performance of the hybrid elements compared to the equivalent displacement formulated elements. The hybrid elements are especially designed for very slender situations. Stresses between the hybrid formulated and equivalent displacement formulated elements are exactly the same, except in the case where a linear interpolation scheme was used. The computational efficiency of the hybrid elements above the equivalent displacement formulated elements is very important.

In the case of a dynamic analysis, quite the contrary is true: the displacement formulated elements are now cheaper than the associated hybrid formulated elements, and the stresses obtained with cubic interpolation are more conservative than stresses obtained with linear interpolation. Results obtained in the dynamic analysis are shown in Table 5.3. It is important to note that these results are for a case where no fluid was present, since only the B21 element could yield results when fluid forces were specified.

Element Type	Theory	Formulation	Intepolation	Nodes
B21	Timoshenko	Displacement	Linear	2
B21H	Timoshenko	Hybrid	Linear	2
B22	Timoshenko	Displacement	Quadratic	3
B22H	Timoshenko	Hybrid	Quadratic	3
B23	Bernoulli	Displacement	Cubic	2
B23H	Bernoulli	Hybrid	Cubic	2

Table 5.1: Definition of Codes Used for Different Element Types

Element Type	Time	Maximum Bending Moments	
See Table 5.1	% of Longest Time	Sagbend (MNm)	Overbend (MNm)
B21	51	-7.0064	17.321
B21H	34	-7.1073	17.904
B22	100	-7.0562	18.121
B22H	58	-7.0562	18.121
B23	95	-7.0622	20.258
B23H	46	-7.0622	20.258

Table 5.2: Performance of Different Element Types in the Static Analysis

Element Type	Time	Maximum Bending Moments	
See Table 5.1	% of Longest Time	Sagbend (MNm)	Overbend (MNm)
B21	5.1	-9.980	20.72
B21H	7.6	-9.770	20.44
B23	27.4	-9.820	19.82
B23H	100	-15.15	20.26

Table 5.3: Performance of Different Element Types in the Dynamic Analysis

Element Type	Time	Increment (% of Total)	
See Table 5.1	% of Longest Time	First	Last
B21	100	0.03	33.0
B21H	62	0.1	29.2

Table 5.4: Performance between Displacement Formulated and Hybrid Formulated Elements

Details about the increment sizes and execution time of hybrid and displacement formulated elements are compared in Table 5.4.

In the previous discussion, analyses were compared where the same number of elements was used, but where the number of interpolation points differed. To compare the performance between element types where the same number of interpolation points was used, a model of 21 B21 elements was compared with a 7 B23 element model. Figure 5.1 shows that bending moments obtained in the seabed region differ considerably, but since these moments are close to zero, it is not problematic. Figure 5.2 compares displacements. In this case the results differ slightly since displacements are calculated at 22 points in the B21 model and only at 8 points in the B23 model. Interesting to note is that the B23 elements are now cheaper (48 % cheaper) to run than the B21 elements.

A comparison of stresses and execution time between models where the mesh was refined with a factor of 5 showed only a 1 % difference in the maximum sagbend moment and a considerable increase in runtime, and a relative coarse mesh (element length/total length ≈ 0.05) will yield sufficient accuracy.

5.1.3 The Influence of Drag

The selection of a suitable drag coefficient is yet another uncertainty. Figure 5.3 compares the maximum bending moment (expressed as a percentage of the bending moment obtained when no drag is used) with different drag coefficients. From literature it is evident that typical drag coefficients vary between 0.6 and 1.1. If a slight error is made with the chosen coefficient in this range, the resulting error in bending stress will be small. A slight error of drag coefficient in the range between 0 and 0.3 will, however, result in a significant difference in stresses. Fortunately, this range is normally not of interest. Another important observation is that a lower drag coefficient

Element Type	Analysis Steps	Time	Increment (% of Total)	
See Table 5.1		% of Longest Time	First	Last
B21	1	100	0.03	33.0
B21	2	47	6.80	34.4
B21H	1	62	0.10	29.2
B21H	2	45	10.0	33.8

Table 5.5: Performance between Displacement Formulated and Hybrid Formulated Elements using 1 or 2 Analysis Steps

will always yield more conservative results. The reason for this is that the drag force damps out motion and the higher the drag coefficient, the more damping will occur.

5.2 LOADING SPECIFICATION

5.2.1 How to Apply The Loads

As mentioned before, the small flexibility of the pipe causes convergence difficulties in the beginning of the analysis. A considerable gain in performance is possible if the structure is stiffened with the barge tension before the remaining loads are applied. Table 5.5 shows the the performance between an analysis where all the loads are applied similtaneously and where they are applied in two analysis or history steps. In addition, the performance of the hybrid formulated elements are also shown. The following observations can be made:

1. A considerable gain in performance is evident when the structure is stiffened with the barge tension before the remaining loads are applied.
2. The gain is less significant for the hybrid elements since these elements use the axial load as an independent unknown.
3. The performance of a displacement and hybrid formulated element is approximately the same if two analysis steps are used.

Figure 5.4, where the fraction of the step completed is plotted against the increment number divided by the total number of increments, show these

observations graphically. The solid lines show the performance of the displacement formulated elements and the dotted lines the hybrid's, while a thin line represents performance in one step and the bold line the performance in two steps.

5.2.2 Influence of Tolerances

Equilibrium within an element is satisfied when all the forces fall below a specified tolerance, and accuracy is primarily influenced by the size of the tolerances. A moment tolerance can also be specified, but it has been observed that the horizontal and vertical forces are the critical forces (the last forces to fall below the specified tolerance) and that the moment residual is usually very small once a solution is accepted.

Table 5.6 shows the effect of force tolerances (expressed as a percentage of the axial force) on the performance of a B21 element. A change of tolerance from 0.001 % to 10 % reduces the execution time considerably, but the effect on stresses is negligible. The conclusion is that even large force tolerances will yield sufficient accuracy with a considerable saving in execution time.

Tolerance	Time	Maximum Bending Moments	
% of Barge Tension	% of Longest Time	Sagbend (MNm)	Overbend (MNm)
0.001	100	-7.0499	37.9098
0.1	79	-7.0517	37.9128
1.0	54	-7.0532	37.9154
10	18	-7.0645	37.9365

Table 5.6: Effect of Force Tolerance on Execution Time and Maximum Stresses

To envoke automatic time stepping in the dynamic analysis, the half-step residual must be specified. This parameter, in addition to the force tolerance, controls the accuracy of the results. Table 5.7 shows the effect of the half-step tolerance on the performance of the element.

5.2.3 Other Considerations

To keep the analysis within bounds, certain specifications regarding the number of increments allowed and the maximum and minimum sizes of the increments must be specified. If these bounds are exceeded, the analysis will be terminated. For instance: if a solution tends to diverge, increment sizes will automatically be reduced till a sufficiently small increment is found which will enable convergence. If the minimum increment size specified is too small, an erroneous run may continue unnecessarily long before it terminates. It has been found that an analysis was usually erroneous if the increment size reduced below 0.001 % of the total increment.

Other measures that can be taken to prevent an ill conditioned analysis to continue for too long is the maximum number of increments allowed in a step, and the maximum number of iterations allowed within an increment, both values being dependent on the tightness of the tolerances, and the size of increments. Most static analysis steps are solved within 40 increments and equilibrium within an increment is usually reached after 3 to 7 iterations; even if tight force tolerances are used.

In the dynamic case, the maximum number of increments depends on the length of the time history. Equilibruim is usually reached within 2 to 5 iterations.

It is recommended to use automatic integration, especially when all the loads are applied in one step, since the increment sizes can vary dramatically (see Table 5.5). If an analysis is performed by stiffening the structure before application of the remaining loads, the difference between the first and last increment size is smaller, and user specified integration may yield quicker results.

Good practice is to save all the data so that a restart analysis can be performed should the initial analysis terminate due to some unforeseen event.

5.3 CONCLUSION

Performance on the one hand and accuracy on the other, are the two most important considerations in any analysis. This study has shown that bending stresses are fairly insensitive to large tolerances, coarse meshes and different element types, but a considerable gain in performance is possible by proper

selection of these factors.

Tighter tolerances and refined meshes can always be employed once all the complications have been eliminated and confidence with the model has been gained.

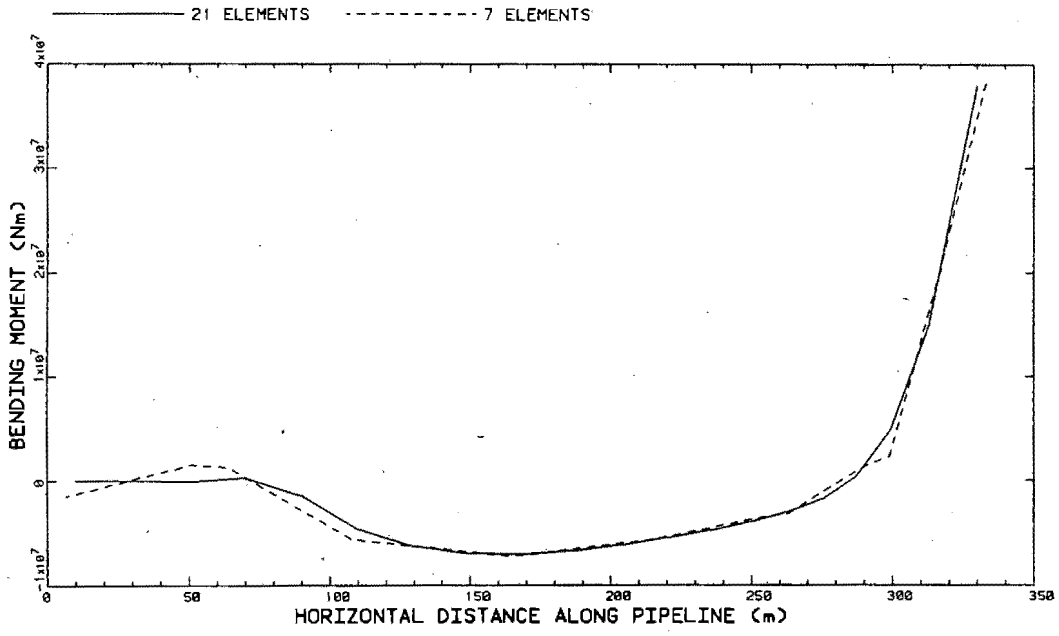

Figure 5.1: Bending Moment Difference between 21 B21 and 7 B23 Elements

Tolerance	Time	Maximum Bending Moments	
Times Barge Tension	% of Longest Time	Sagbend (MNm)	Overbend (MNm)
10^9	22.2	-8.486	18.63
10^4	22.7	-8.486	18.63
10^2	29.5	-8.322	18.96
1	100	-8.284	19.09

Table 5.7: Effect of Half-step Tolerance on Performance

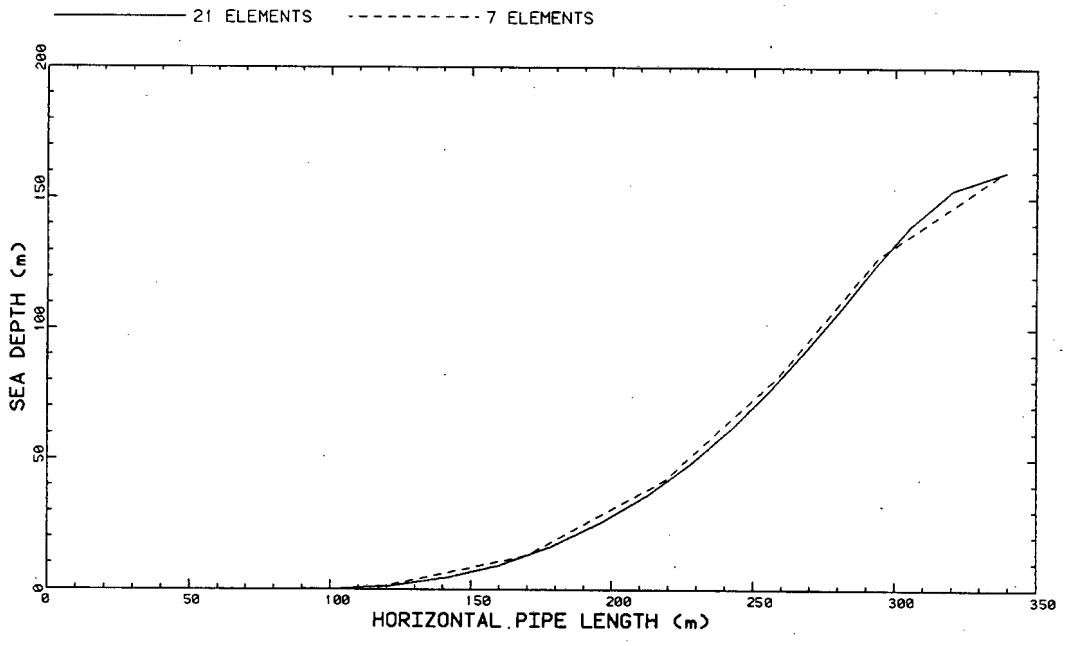

Figure 5.2: Displacement Difference between 21 B21 and 7 B23 Elements

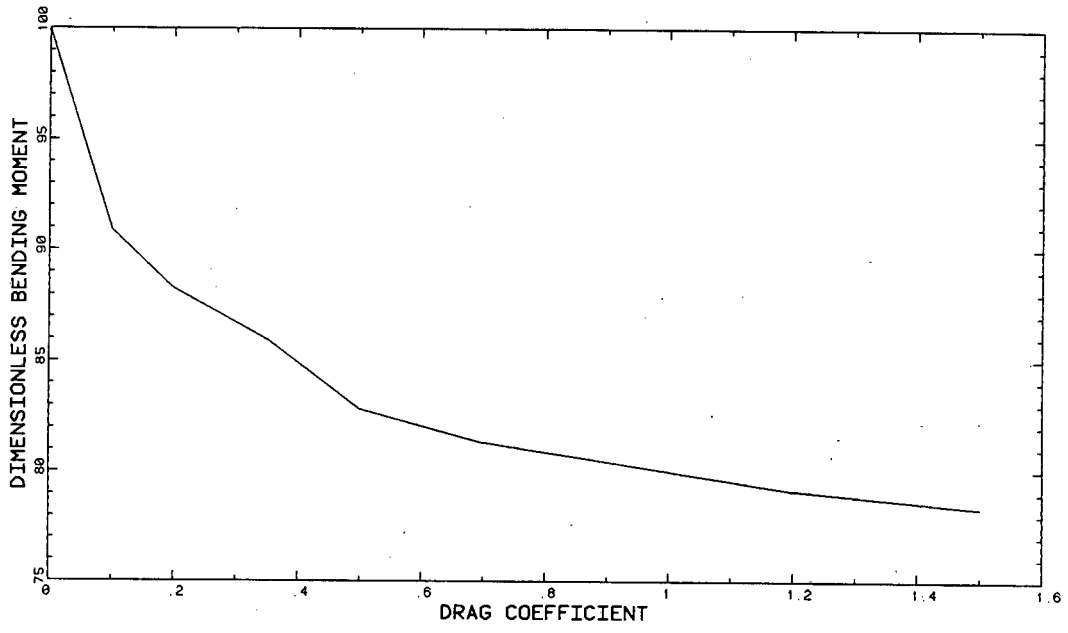

Figure 5.3: Influence of Drag Coefficient on Bending Moment as Fraction of Bending Moment Obtained without Drag

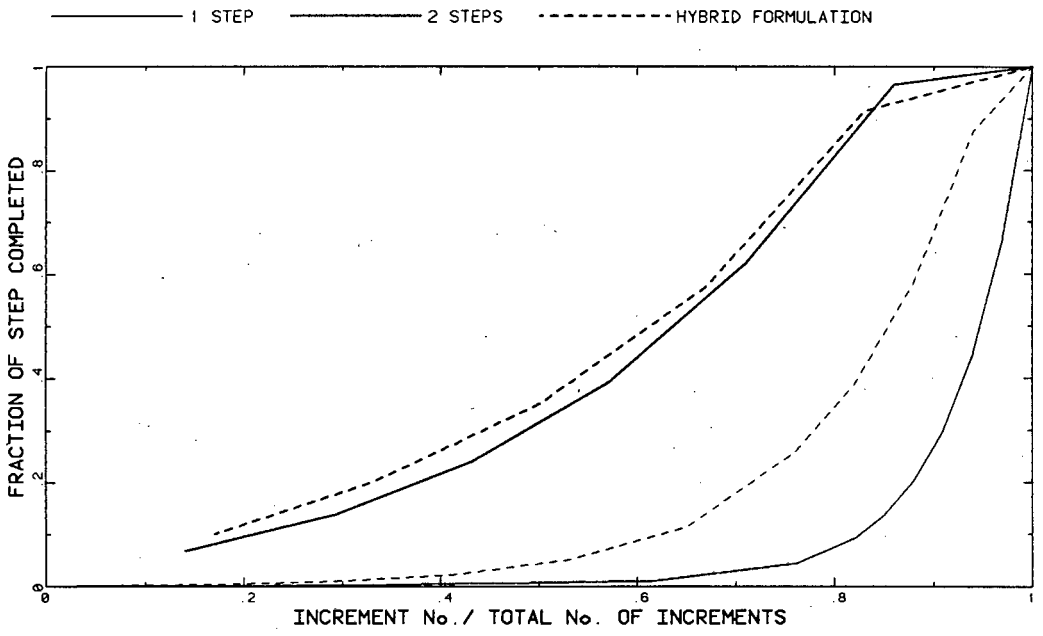

Figure 5.4: Performance between an Analysis using 1 or 2 Analysis Steps and Different Formulations

6 SUMMARY

The objective of this thesis was to contribute to the expertise of the South African offshore technology. This was achieved by a summary of the literature on the mechanical and computational aspects conserned. In addition, a number of numerical experiments and parameter studies were performed to obtain experience with some aspects of the problem and to report on the suitability of ABAQUS to model the important aspects of the pipelaying problem.

Analysis of the pipelaying problem is characterised by the flexibility of the pipe, contact of the pipe at both the seabed and stinger, the unknown suspended pipe length at the beginning of the analyses, and complexities arising from fluid-structure interaction. Since closed form solutions are possible for simple cases only, a numerical analysis must be performed. ABAQUS, a nonlinear finite element code, was used in this study to analyse the problem.

The small bending stiffness of the pipe and the large sea depths in which these pipelines are laid result in large pipe displacements and rotations. The solution algorithm used in ABAQUS handles this nonlinearity very well, but equilibrium is obtained much quicker if the pipeline is stiffened with the barge tension before the remaining loads are applied.

Contact between two bodies are accomplished by defining special *contact* elements between them. Only rigid surface and gap elements are suitable in offshore studies. Modelling the seabed as a rigid surface is preferred to using gap elements in most applications, since difficulties can be experienced when gap elements and a fluid are combined in a dynamic analysis. It is, however, impractical to use rigid surface elements to model the stinger in a dynamic analysis, and an alternative model, where equivalent forces are applied at the stinger locations, yielded conservative results.

The unknown suspended length of the pipeline causes a complication in the model when a physical model of the stinger must be included. Since the barge end of the pipeline is free to move in a horizontal direction, defining the stinger at an exact location is difficult. This problem can be solved if the stinger is constrained to match the motion of the barge end of the pipe.

Fluid-structure interaction is characterised by drag and added inertia effects. These forces play a significant role, and must be included in the analysis. The algorithm required to include these forces is complex, and in some cases

difficulties in obtaining solutions for relatively simple cases were experienced. This is especially the case with the dynamic loading.

ABAQUS Version 4.6 has proven itself to be a very powerful tool, especially regarding the solution of nonlinearities arising from large displacements. Special purpose finite element codes may, however, be more convenient to model the fluid-structure interactions.

This thesis has concentrated on modelling the conventional laybarge method. Only the global response of the pipeline due to environmental loads was considered. Localised effects such as buckling of the pipeline or ovalisation of the cross-section is usually a problem, and future studies may be directed to include these effects. Other possibilities are a three-dimensional analysis (which may reveal other numerical problems) where currents and waves out of the pipe plane are introduced, and to account for random rather than harmonic sea states.

Since most of the design graphs available are based on linear dynamic analysis, nonlinear dynamic effects can now be accounted for with the use of ABAQUS. This will essentially entail a parametric study, where different combinations of barge tension, sea depth, pipe data and sea states are compared.

References

[1] ANGRILLI, F. and BERGMASCHI, S. *"On the lateral instability of precurved pipelines"*. Journal of Energy Resources and Technology, Sept. 1980, Vol 102, pp 123.

[2] BATHE, K.J. *"Finite element procedures in engineering analysis"* Prentice-Hall, Inc. 1982. pp 65-112,301-313.

[3] BATHE, K.J. and WILSON, E.L. *"Numerical methods in finite element analysis"* Prentice-Hall, Inc. 1976. pp 308-342.

[4] BELYTSCKO, T. and HUGHES, T.J.R. *"Computation methods for transient analysis, Vol. 1"* Elsevier Science Publishers B.V., 1983 pp 2-155.

[5] BERGAN, P.G. and MOLLESTAD, E. *"Impact - response behaviour of offshore pipelines"*. Journal of Energy Resources and Technology, Dec. 1982, Vol. 104, pp 325.

[6] BERGAN, P.G. and MOLLESTAD, E. *"Nonlinear dynamic analysis of submerged pipelines"*. Computer methods in Applied Mechanics and Engineering, 1982, Vol. 32, pp 881.

[7] BRANDO, P. and SEBASTIANI, G. *"Determination of sealines elastic curves and stresses to be expected during laying operations"*. Offshore Technology Conference, Houston. 1971, Paper OTC 1354.

[8] BREBBIA, C.A. and WALKER, S. *"Dynamic analysis of offshore structures"* Newnes-Butterwoths, London. pp 1-13,61-144.

[9] BREWER, W.V. and DIXON, D.A. *"Influence of laybarge motions on a deepwater pipeline laid under tension"*. Journal of Engineering for Industry, Aug. 1970, pp 595.

[10] BROWN, M.J. and ELLIOTT, L. *"Pipelaying from a barge"*. Math. Engng Ind. Vol 1,No 1, pp 32.

[11] BRYNDUM, M.B. and COLQUHOUN, R.S. *"Dynamic lay stresses for pipelines"*. Offshore Technology Conference, Houston. 1982, Paper OTC 4267, pp 469.

[12] CHUNG, J.S. and FELIPPA, C.A. *"Nonlinear static analysis of deep ocean mining pipe - Part i and ii"* Journal of Energy Resources Technology, March 1981, Vol. 103, pp 11.

[13] CLOUGH, R.W. and PENZIEN, J.P. *"Dynamics of structures"*. McGraw-Hill, Inc. 1975.

[14] COWAN, R. and ANDRIS, R.P *"Total pipelaying system dynamics"*. Offshore Technology Conference, Houston. 1977, Paper OTC 2914, pp 291.

[15] DAREING, D.W. and NEATHERY, R.F. *"Marine pipline analysis based on Newtons method with an artic application"*. Journal of Engineering for Industry, Nov. 1970, pp 827.

[16] DATTA, T.K. and BASU, A.K. *"Stress analysis of submarine pipelines"*. Proceedings of Institute for Civil Engineers,Part 2, Dec 1977, pp 833.

[17] DATTA, T.K. *"Abandonment and recovery solution of submarine pipelines"*. Applied Ocean Research, 1982, Vol. 4,No. 4, pp 247.

[18] DESAI, C.S. and CHANDRAKANT, S. *"Introduction to the Finite Element Method"*. Van Nostrand Reinhold Company, 1972, pp 215-244.

[19] DIXON, D.A. and RUTHLEDGE, D.R. *"Stiffened catenary calculations in pipeline laying problem"*. Journal of Engineering for Industry, Feb 1986, pp 153.

[20] FELIPPA, C.A. and CHUNG, J.S. *"Nonlinear static analysis of deep ocean mining pipe-Part i and ii"*. Journal of Energy Resources and Technology, March 1981, pp 11.

[21] FERTIS, D.G. *"Dynamics and Vibrations of structures"* John Wiley and Sons, 1973.

[22] GALLAGER, R.H. *"Finite element analysis"*. Prentice-Hall, Inc. 1975, pp 108-188.

[23] GARRET, D.L. *"Dynamic analysis of slender rods"*. Journal of Energy Resources and Technology, Dec 1982, pp 302.

[24] HALL, J.E. and HEALEY, A.J. *"An analytical study of controlled buoyancy laying deep-sea pipelines"*. Journal of Engineering for Industry, Feb. 1975, pp 266.

[25] HALL, J.E. and HEALEY, A.J. *"Dynamics of suspended marine pipelines"*. Journal of Energy Resources and Technology, June 1980, Vol 102, pp 112.

[26] HALLAM, M.G., HEAF, N.J. and WOOTON, L.R. *"Dynamics of marine structures: Methods of calculating the dynamic response of fixed structures subject to wave and current action"*. Cira Underwater Engineering Group, Report No. UR 8, 1978.

[27] HIBBITT, KARLSSON and SORENSON. *"ABAQUS users manual"* 1987.

[28] HIBBITT, KARLSSON and SORENSON. *"ABAQUS theory manual"* 1987.

[29] HIBBITT, KARLSSON and SORENSON. *"ABAQUS examples manual"* 1987.

[30] KAN, W.C. and HEALEY, A.J. *"Finite element analysis with the state variable transfer matrix and geometric nonlinearity for marine pipelines in subsurface tow"*. Journal of Energy Resources and Technology, March 1981, Vol 103, pp 27.

[31] KARAL, K and HALVORSEN, S.A. *"Dynamics of the water-pipeline-soil interaction"*. Journal of Energy Resources and Technology, Dec. 1982, Vol. 104, pp 307.

[32] KIRK, C.L. and ETOK, E.U. *"Wave induced random oscillations of pipelines during laying"*. Applied Ocean Research, 1979, Vol. 1. No. 1, pp 51.

[33] KONUK, I. *"Higher order approximations in stress analysis of submarine pipelines"*. Journal of Energy Resources and Technology, Dec. 1980, pp 190.

[34] KONUK, I. *"Application of an adaptive numerical technique to 3-D pipeline problems with strong nonlinearities"*. Journal of Energy Resources and Technology, March 1982, pp 58.

[35] LARSEN, C.M. *"Static and dynamic analysis of offshore pipelines during installation"*. The Norwegian Institute of Technology, Dec. 1976, Report SK/M 35.

[36] MAIER, G. et al. *"Optimization of stringer geometry for deepsea pipelaying"*. Journal of Energy Resources and Technology, Dec. 1982, Vol. 104, pp 295.

[37] MATTEELLI, R., ANDREUZZI, F. and TADDEI, F. *"Sea-line laying in deep waters"*. Offshore Technology Conference, Houston 1976, Paper OTC 2677, pp 695.

[38] McCORMIC, M. *"Ocean engineering and mechanics"*. John Wiley and Sons, 1973. pp 24-61,78-85.

[39] NOOR, A.K. and PILKEY, W.D. *"State of the Art surveys on Finite Element Technology"* American Society of Mechanical Engineers Company, 1983. pp 127-162,405-450.

[40] OVUNC, B. and MALLAREDDY, U. *"Stress analysis of offshore pipelines under dynamic loads"*. Offshore Technology Conference, Houston. 1971, Paper OTC 1361, pp 1349.

[41] PALMER, A.C., HUTCHINSON,G. and ELLIS, J.W. *"Configuration of submarine pipelines during laying operations'*. Journal of Engineering for Industry, Nov. 1974, pp 1112.

[42] PALMER, A.C. *"Analysis and behaviour of pipelines during installation"*. Behaviour of Offshore Structures - The Norwegian Instutite of Technology. BOSS 1976, pp 113.

[43] PAZ, M. *"Structural Dynamics (Theory and computation)"* Van Nostrand Reinhold Company, 1980.

[44] PEDERSON, P.T. *"Equilibrium of offshore cables and pipelines during laying"*. International Ship Building Research, 1975, Vol. 22, pp 399.

[45] PLUNKETT, R. *"Static bending stresses in catenaries and drill strings"*. Journal of Engineering for Industry, Feb. 1967, pp 31.

[46] RAMMANT, J.P. and BACKX, E. *"Offshore pipeline installation sensitivity analysis for conventional laybarge"*. Applied Ocean Research, 1980, Vol 2, No. 1, pp 13.

[47] SUZUKI, N. and JINGU, N. *"Dynamic behaviour of submarine pipelines under laying operation"*. Journal of Energy Resources and Technology, Dec. 1982, Vol. 104, pp 313.

[48] WALLIS, J.R. et al. *"Fatigue analysis of offshore structures"*. Journal of Energy Resources Technology, Dec. 1979, Vol. 101, pp 219.

[49] WILHOIT, J.C. and MERWIN, J.D. *Pipe stresses induced in laying offshore pipelines.* Journal of Engineering for Industry, Feb. 1967, pp 37.

[50] ZIENKIEWIECZ, O.C. *"The finite element method (third edition)"*. McGraw-Hill Book Company, 1977, pp 500-568.

[51] ZUGG, J.B. *"The analysis of offshore pipelines during laying operations"*. B.Sc.(Eng) Thesis. Department Civil Engineering, University of Cape Town, 1986.

A APPENDIX

A.1 AN EXAMPLE OF A GAS-PIPELINE IN S.A. WATERS

A.1.1 The Model

The following data were obtained from industry:

Pipe Outside Diameter	457.2 mm
Wall Tickness	14.27 mm
Coating Thickness	50.0 mm
Coating Density	3050 Kg/m^3
Stinger Length	60 m
Sea Depth	100 m
Tensioner Capasity	2000 KN
Wave Height	7.0 m
Current Velocity	0.4 m/s

The following assumptions were made to complete the model:

Steel Density	7830 Kg/m^3
Youngs Modulus	200 GPa
Water Density	1025 Kg/m^3
Wave period	12.6 *sec.*
Transverse Drag Coefficient	0.7
Tangential Drag Coefficient	0.1
Inertia Coefficient	1.5
Equivalent Stinger reactions	40 KN
Barge tension	500 KN

The concrete coating provides additional weight, but does not contribute to the total stiffness. This is because the pipe is under tension during the laying operation.

Only 25 % of the tensioner's capacity is used as the barge tension force.

The barge motions consits of a harmonic heave motion which is in phase with, and has the same height (7 m) and period (12.6 *sec*), as the wave.

From calculations it is evident that:

Self Weight	3910 N/m
Buoyancy Force (empty pipe)	1000 N/m
Submerged Weight	2910 N/m
Average Density	4000 Kg/m^3

A 400 m pipeline is defined at the sea surface (elevation 100 m) and is modelled using 20 B21 elements. Since the stinger is 60 m long and assumed to have 12 rollers at 5 m distances, each pipe element in the stinger region is futher sub-discretized into 4 elements (see Fig. A.1).

The seabed is modelled as a rigid surface, with its reference node (node 100) specified at the origin. This node must be kept fixed throughout the analysis. To establish contact between the pipe and rigid surface, IRS21 interface elements (element numbers 51 to 68) are specified with the same node numbers as the pipeline.

The pipe is initially free to move horizontally at the barge end (node 30), and can move vertically and rotate at the other end (node 1). After the static profile is determined, the boundary conditions are changed to account for dynamic barge motions. The prescribed barge motion is defined in a user-subroutine. Alternatively, the required motion can be specified with the use of the amplitude (where the motion is expressed with a Fourier series) option.

The pipe is stiffened with the barge tension in the first history step. This is a linear process, but it is important to request a large displacement analysis rather than a linear small displacement analysis, since a linear analysis is not allowed when contact elements are specified. The force tolerance is taken as 2 % of the barge tension, and is considered small enough to yield accutate results. The same force tolerance is then used throughout the analysis.

The self weight, buoyancy and drag forces are applied in the second step. After an initial displaced curve is obtained, the reaction forces at the roller locations are applied, and a new static profile is determined. The dynamic response is then obtained in the final history step.

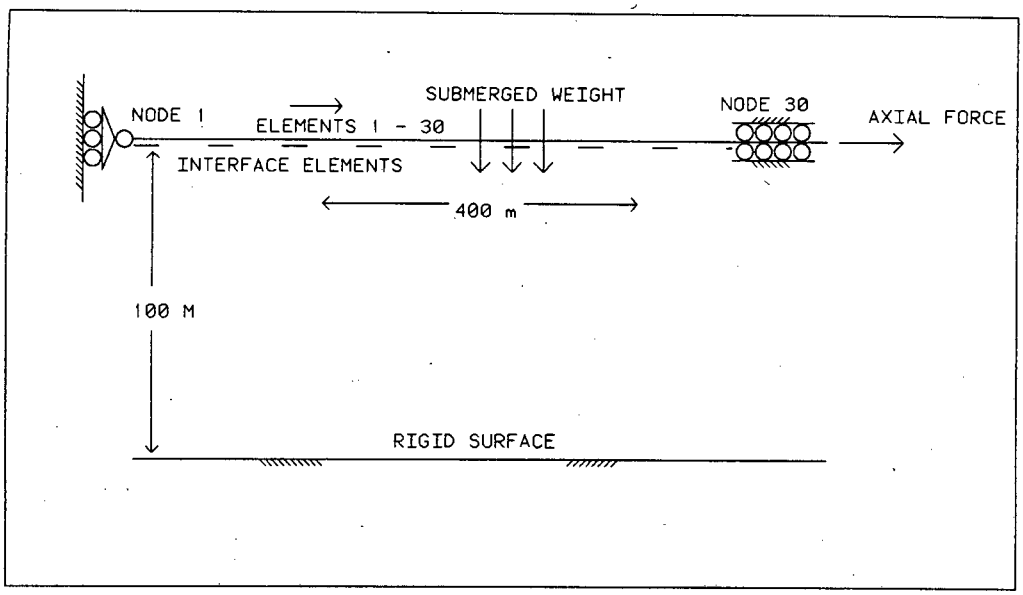

Figure A.1: Finite Element Model

A.1.2 Input Data and Results

The following ABAQUS input specification is required:

```
*HEADING
ANALYSIS OF A GAS-PIPELINE IN SOUTH AFRICAN WATERS
*PREPRINT,ECHO=YES,HISTORY=YES,MODEL=YES
*RESTART,WRITE,FREQ=10
*NODE
1,0.0,100.0
18,340.0,100.0
19,345.0,100.0
30,400.0,100.0
100,0.0,0.0
*NGEN,NSET=PIPE
1,18
19,30
*NSET,GENERATE,NSET=STINGER
18,29
*ELEMENT,TYPE=B21
1,1,2
*ELGEN,ELSET=PIPE
```

```
1,29
*ELEMENT,TYPE=IRS21
51,1,2,100
*ELGEN,ELSET=SEABED
51,17
*BEAM GENERAL SECTION,SECTION=PIPE,ELSET=PIPE,DENSITY=4000
0.2286,0.01427
0.0,0.0,-1.0
200.0E9
*RIGID SURFACE,TYPE=SEGMENTS,ELSET=SEABED
START,0.0,0.0
LINE,400.0,0.0
*INTERFACE,ELSET=SEABED
*FRICTION
0.5,50.0E3
*AQUA
0.0,100.0,9.81,1025.0
0.0,0.0,0.0,0.0
0.4,0.0,0.0,100.0
*WAVE,TYPE=STOKES
7.0,12.6,0.0,1.0
**
*USER SUBROUTINE
      SUBROUTINE DISP(U,KSTEP,KINC,TIME,NODE,JDOF)
      IMPLICIT REAL*8(A-H,O-Z)
      FREQ=0.5
      HEIGHT=7.0
      U=0.5*HEIGHT*SIN(FREQ*TIME)
      RETURN
      END
** ----------------------------------------------------------------
*STEP,NLGEOM,INC=10,CYCLE=5
STIFFEN PIPE WITH BARGE TENSION
*STATIC,PTOL=10000
*CLOAD
30,1,500.0E3
*BOUNDARY
1,1
30,2
30,6
100,ENCASTRE
*EL PRINT,FREQ=100
SF
S
```

```
*NODE PRINT,FREQ=100
U
COORD
*END STEP
** ----------------------------------------------------------------
*STEP,NLGEOM,INC=30,CYCLE=15
ADD SELF WEIGHT, BOUYANCY AND DRAG
*STATIC,PTOL=10000
0.1,1.0,1.0E-4
*DLOAD
PIPE,PY,-3910.
PIPE,PB,,0.5572
PIPE,PD,,0.5572,0.7,0.1,1.5
*END STEP
** ----------------------------------------------------------------
*STEP,NLGEOM,INC=15,CYCLE=15
ADD EQUIVALENT STINGER REACTIONS
*STATIC,PTOL=10000
0.1,1.0,1.0E-4
*CLOAD
STINGER,2,40.0E3
*END STEP
** ----------------------------------------------------------------
*STEP,INC=500,CYCLE=10
EXCITE PIPE WITH BARGE MOTIONS AND WAVES
*DYNAMIC,HALFTOL=1.0E10,PTOL=10000
0.01,20.0,1.0E-4,1.0
*BOUNDARY,OP=NEW
1,1
30,6
100,ENCASTRE
*BOUNDARY,USER SUB,OP=NEW
30,2
*EL FILE
SF
S
*NODE FILE
U
COORD
*END STEP
** ----------------------------------------------------------------
```

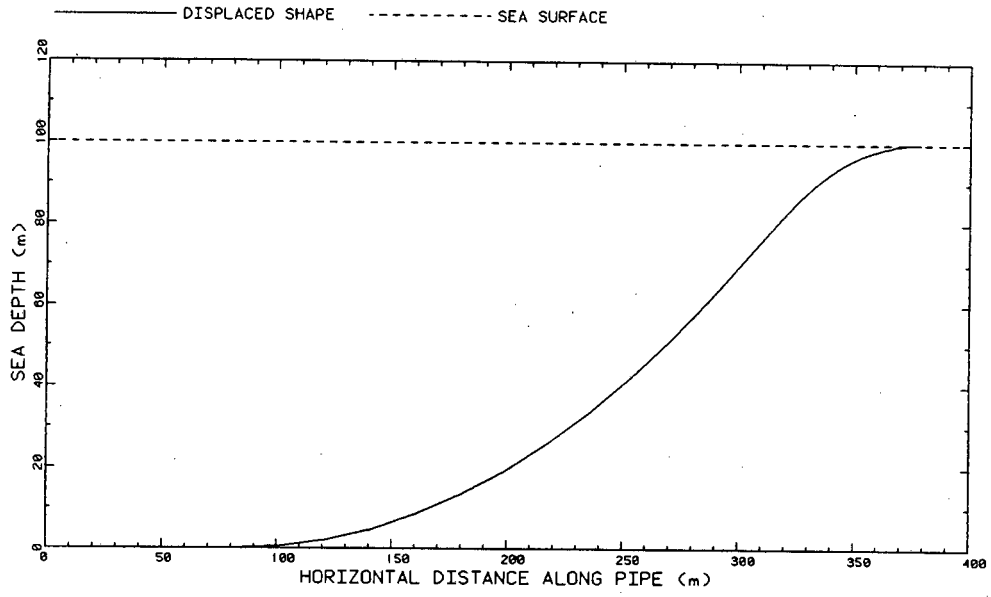

Figure A.2: Static Displaced Shape

Figure A.2 shows the static displaced shape of the pipeline (eg. configuration after analysis step 3), and the bending moment envelope relative to the static moments is shown in Figure A.3.

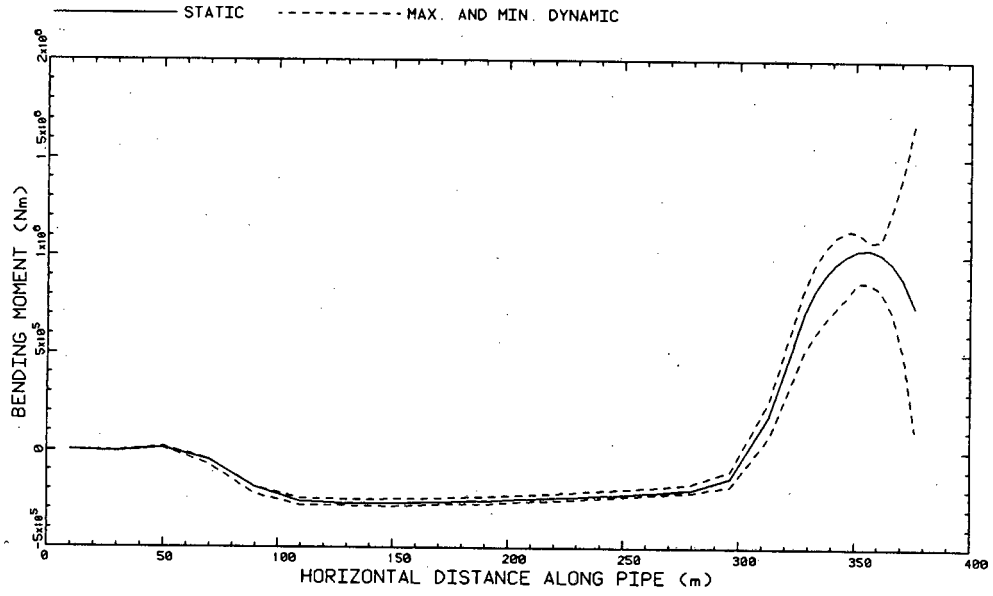

Figure A.3: Bending Moment Envelope